49 Leri A, Claudio PP, Li Q, *et al.* Stretch-mediated release of angiotensin II induces myocyte apoptosis by activating p53 that enhances the local renin-angiotensin system and decreases the Bcl-2-to-Bax protein ratio in the cell. J Clin Invest 1998;101:1326–1342.
50 Aikawa R, Komuro I, Yamazaki T, *et al.* Oxidative stress activates extracellular signal-regulated kinases through Src and Ras in cultured cardiac myocytes of neonatal rats. J Clin Invest 1997;100:1813–1821.
51 Slater AF, Stefan C, Nobel I, *et al.* Signalling mechanisms and oxidative stress in apoptosis. Toxicol Lett 1995;82-83:149–153.
52 Gerschenson LE, Rotello RJ. Apoptosis: a different type of cell death. FASEB J 1992;6:2450–2455.
53 Korsmeyer SJ. Regulators of cell death. Trends Genet 1995;11:101–105.
54 Matsushita K, Okita H, Suzuki A, *et al.* Islet cell hyperplasia in transgenic mice overexpressing EAT/mcl-1, a bcl-2 related gene. Mol Cell Endocrinol 2003;203:105–116.
55 Shimizu S, Eguchi Y, Kamiike W, *et al.* Bcl-2 blocks loss of mitochondrial membrane potential while ICE inhibitors act at a different step during inhibition of death induced by respiratory chain inhibitors. Oncogene 1996;13:21–29.
56 Shimizu S, Eguchi Y, Kamiike W, *et al.* Retardation of chemical hypoxia-induced necrotic cell death by Bcl-2 and ICE inhibitors: possible involvement of common mediators in apoptotic and necrotic signal transductions. Oncogene 1996;12:2045–2050.
57 Deten A, Volz HC, Briest W, *et al.* Cardiac cytokine expression is upregulated in the acute phase after myocardial infarction. Experimental studies in rats. Cardiovasc Res 2002;55:329–340.
58 Frangogiannis NG, Youker KA, Rossen RD, *et al.* Cytokines and the microcirculation in ischemia and reperfusion. J Mol Cell Cardiol 1998;30:2567–2576.
59 Kukielka GL, Smith CW, Manning AM, *et al.* Induction of interleukin-6 synthesis in the myocardium. Potential role in postreperfusion inflammatory injury. Circulation 1995;92:1866–1875.
60 Sawa Y, Ichikawa H, Kagisaki K, *et al.* Interleukin-6 derived from hypoxic myocytes promotes neutrophil-mediated reperfusion injury in myocardium. J Thorac Cardiovasc Surg 1998;116:511–517.
61 Ohtsuka T, Hamada M, Inoue K, *et al.* Relation of circulating interleukin-6 to left ventricular remodeling in patients with reperfused anterior myocardial infarction. Clin Cardiol 2004;27:417–420.
62 Hajjar RJ, Schmidt U, Matsui T, *et al.* Modulation of ventricular function through gene transfer *in vivo*. Proc Natl Acad Sci USA 1998;95:5251–5256.
63 Peters M, Blinn G, Solem F, *et al. In vivo* and *in vitro* activities of the gp130-stimulating designer cytokine Hyper-IL-6. J Immunol 1998;161:3575–3581.

Available online at www.sciencedirect.com
SCIENCE DIRECT
Biochimica et Biophysica Acta 1725 (2005) 57 – 63
BIOCHIMICA ET BIOPHYSICA ACTA
BBA
http://www.elsevier.com/locate/bba

Membranous osteogenesis system modeled with KUSA-A1 mature osteoblasts

Satoshi Matsumoto[a,d], Isao Shibuya[a], Satoshi Kusakari[b], Kaoru Segawa[c], Taro Uyama[a], Akinori Shimada[d], Akihiro Umezawa[a,*]

[a]*Department of Reproductive Biology and Pathology, National Institute for Child Health and Development, 2-10-1 Okura, Setagaya-ku, Tokyo 157-8535, Japan*
[b]*Department of Pathology, Keio University School of Medicine, Tokyo 160-8582, Japan*
[c]*Department of Microbiology and Immunology, Keio University School of Medicine, Tokyo 160-8582, Japan*
[d]*Department of Veterinary Pathology, Tottori University, Tottori 680-8553, Japan*

Received 22 September 2004; received in revised form 16 May 2005; accepted 17 May 2005
Available online 17 June 2005

Abstract

Several stromal cells were established from murine bone marrow cultures. One of the KUSA subclones, KUSA-A1 cells, displays osteogenic characteristics in vitro and in vivo. The calcium deposition, osteocalcin release, and parathyroid hormone (PTH) responsiveness of KUSA-A1 cells indicate that they are mature osteoblasts or osteocytes. Bone had formed in subcutaneous tissue 1 week after subcutaneous injection of cells into immunodeficient mice. The osteogenesis by KUSA-A1 was not mediated by chondrogenesis and thus was considered to be membranous ossification. These unique characteristics of KUSA-A1 cells provide an opportunity to analyze the process of membranous ossification in detail.

Keywords: Membranous osteogenesis; Stromal cell; KUSA; Osteoblast; Gap junction

1. Introduction

The concept of regenerative medicine refers to the cell-mediated restoration of damaged or diseased tissue. Candidate cell sources for tissue regeneration include embryonic stem cells, fetal cells, and adult cells, such as marrow stromal cells [1], each of which has both advantages and drawbacks. Clinical trials with marrow stromal cells have been performed in patients with osteogenesis imperfecta [2] and osteoporosis [3,4], and marrow stromal cells are expected to be a good source of cell therapy [5]. Multipotent mesenchymal stem cells have been isolated from adult marrow and shown to differentiate into multiple cell types, such as osteoblasts, chondrocytes, adipocytes, myoblasts [1,5,6], cardiomyocytes [7,8], endothelial cells, and neuronal cells [9].

In the present study, we characterized a single cloned, immortalized stromal cell line, KUSA-A1, established from murine bone marrow cultures [6]. KUSA-A1 cells are capable of generating mature bone in vivo. They are a unique, mature osteoblast cell line and will serve as a very suitable model for in vivo osteogenesis.

2. Materials and methods

2.1. Cell culture

The stromal cell lines were isolated from long-term bone marrow cultures of C3H/He female mice and cultured as previously described [6,9–11]. Cells were cultured in Iscove's modified Dulbecco's medium (IMDM) supple-

* Corresponding author. Tel.: +81 3 5494 7047; fax: +81 3 5494 7048.
E-mail address: umezawa@1985.jukuin.keio.ac.jp (A. Umezawa).

0304-4165/$ - see front matter © 2005 Elsevier B.V. All rights reserved.
doi:10.1016/j.bbagen.2005.05.027

mented with 20% fetal bovine serum (FBS) and penicillin (100 μg/ml)/streptomycin (250 ng/ml) at 37 °C in humid air with 5% CO_2. Immortalized cells were obtained by frequent subculture for over a year. Cell lines from different dishes were subcloned by limiting dilution. The murine stromal cell lines are summarized in Fig. 1. In vitro calcification assay, osteocalcin production, and evaluation of parathyroid hormone (PTH) response were performed as previously described [10].

2.2. Measurement of alkaline phosphatase (ALP)

KUSA/A1 and MHCTC-E1 cells were analyzed by ALP assay as described [20].

2.3. Communication assay

Intercellular transfer Fluorescent Lucifer Yellow CH (Sigma, St. Louis, Missouri) was measured after the direct microinoculation of the dye into a KUSA-A1 cell as previously described [12,13].

2.4. RNA extraction and Northern blotting

RNA was prepared by homogenizing the specimens in guanidinium isothiocyanate, followed by centrifugation over a cesium chloride cushion as previously described [6,14]. The RNA was then electrophoresed in a 1.0% agarose gel, transferred to a nylon filter, and hybridized with a cDNA insert labeled with ^{32}P-dCTP by the random-primer method at 65 °C for 14–16 h in a buffer containing 5× SSPE (1× SSPE is 0.15 M NaCl, 10 mM NaH_2PO_4/Na_2HPO_4 (pH 7.4), and 1 mM EDTA), 5× Denhardt's solution (1× Denhardt's solution is 0.02% Ficoll polyvinylpyrrolidone and 0.02% BSA), 0.02% poly(A), and 1% SDS. The blots were washed with 2× SSC (1× SSC is 0.15 M NaCl and 0.015 M sodium citrate, pH 7.4) containing 1% SDS at room temperature and 65 °C. Final washing was performed with 0.1× SSC containing 0.1% SDS at 65 °C.

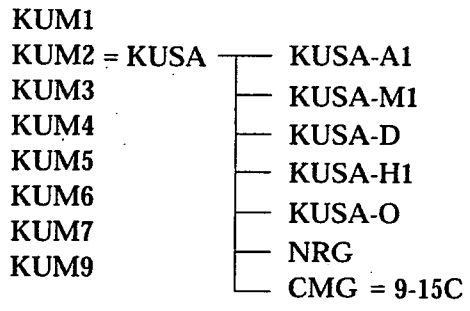

Fig. 1. The murine stromal cell lines. The clonal cells were designated KUM1 [6], KUM2/KUSA [6,9], KUM3-7 [6], and KUM9 [6,9]. The KUSA-A1 [6,11], KUSA-M1 [6], KUSA-D [6], KUSA-H1 [6], KUSA-O [6], and NRG [9] cells were subclones of KUSA cells. The CMG/9-15C cells are a subclone from KUSA cells that had been after exposed to 5-azacytidine [7,11]. The cell names are available at http://1985.jukuin.keio.ac.jp/umezawa/kum/kumh.html.

The blots were exposed to X-ray film at 80 °C with an intensifying screen. RNA blot analysis was carried out as previously described [6,14].

2.5. Transmission electron microscopy (TEM)

KUSA-A1 cells cultured in vitro for 14 days post-confluence were examined by TEM. The samples were fixed in 2.5% glutaraldehyde postfixed in 1% osmium tetroxide. They were rinsed in water, dehydrated, and embedded in epoxy resin. Ultrathin sections (70–90 nm) were cut and stained with 2% uranyl acetate and Reynold's lead citrate before being examined with a JEM-1200 EX microscope (JOEL Co., Japan) at 80 kV.

2.6. Inoculation of cells into mice

To determine the ability of KUSA, KUM3, KUM4, and NIH-3H3 cells to differentiate in vivo, freshly scraped KUSA-MTAg, KUM3-MTAg, KUM4-MTAg, and NIH3T3-MTAg cells (10^7 cells) were subcutaneously inoculated into Balb/c *nu/nu* mice (Sankyo Laboratory, Hamamatsu, Japan) as previously described [6]. Animals were sacrificed by cervical dislocation between 4 and 8 weeks after inoculation.

To determine the potential osteogenic activity of KUSA-A1 cells in vivo, freshly scraped KUSA-A1 cells (10^7 cells) were subcutaneously inoculated into severe combined immunodeficient (SCID) mice (Nippon CLEA, Hamamatsu, Japan). Subcutaneous specimens were resected between 1 and 4 weeks after inoculation and decalcified for a few days in formic acid. The implants were embedded in paraffin. Paraffin sections were deparaffinized, hydrated, and stained with hematoxylin and eosin.

All animals received human care incompliance with the "Principles of Laboratory Animal Care" formulated by the National Society for Medical Research, and the "Guide for the Care and Use of Laboratory Animals" prepared by the Institute of Laboratory Animal Resource and published by the US National Institute of Health (NIH Publication No. 86-23, revised in 1985). The operation protocols were accepted by the Laboratory Animal Care and the Use Committee of the National Research Institute for Child and Health Development, Tokyo, and Keio University School of Medicine.

3. Results

3.1. In vitro characterization of KUSA-A1 cells, single-cell-derived mature osteoblasts

In vitro, calcification by KUSA-A1 cells gradually increased during the culture period (Fig. 2A), and the amount of osteocalcin released into the culture medium also increased (Fig. 2B). The KUSA-A1 cells responded to PTH

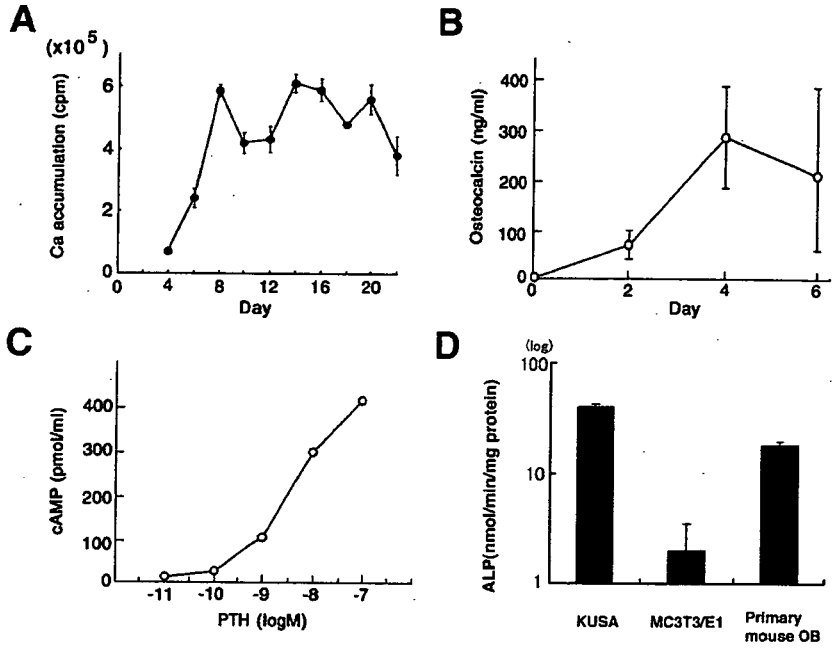

Fig. 2. Characteristics of KUSA-A1 cells as an osteoblast model. (A) Quantitative analysis of calcium deposition by KUSA-A1 cells. (B) Bone Gla protein (Osteocalcin) secretion by KUSA-A1 cells. (C) cAMP production after exposure to PTH. The KUSA-A1 cell response to PTH was assessed by measuring cAMP production. (D) ALP activity in KUSA-A1 cells and MC3T3-E1 cells at 7 days.

in a dose-dependent manner (Fig. 2C). The ALP activity of KUSA-A1 cells was approximately ten-fold higher than in MC3T3-E1 cells at 7 days (Fig. 2D). The calcium deposition and osteocalcin release indicated that KUSA-A1 cells are mature osteoblasts or osteocytes.

3.2. Morphology of KUSA-A1 cells: transmission electron microscopy (TEM) in vitro

Bone nodules [15] that had developed in KUSA-A1 cells cultured in medium supplemented with 10 mM beta-glycerophosphate were fixed and stained in situ by the von Kossa technique (Fig. 3A). The bone nodules consisted of an eosinophilic matrix containing ovoid cells resembling osteocytes, and the KUSA-A1 cells were arranged at the periphery of the nodule in the form of a periosteum-like cell layer. Mineral deposition by the KUSA-A1 cells demonstrated that they have the capacity to differentiate into osteoblasts, to deposit hydroxyapatite in well-developed bone matrix, and to express the differentiated state of osteoblasts.

Ultrastructurally, the matrix was electron-dense and was clearly produced by the cells in the bone nodules (Fig. 3B). The extracellular matrix produced by KUSA-A1 cells was

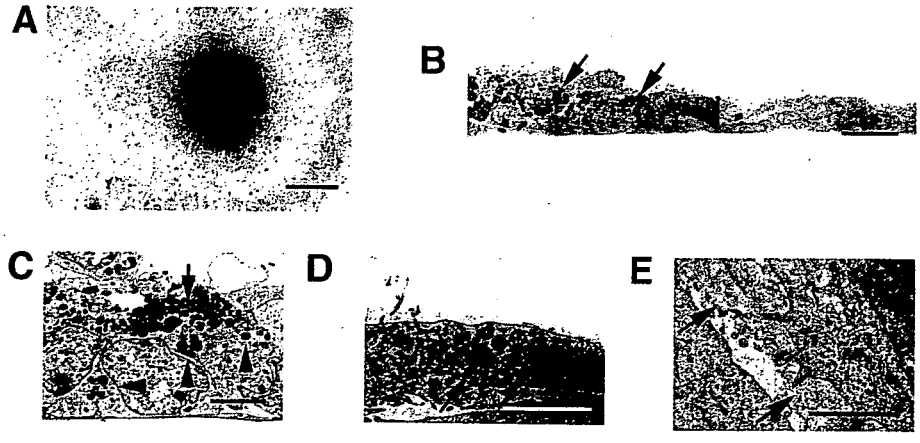

Fig. 3. Ultrastructural analysis of KUSA-A1 cells in culture. (A) KUSA-A1 cells 30 days after confluence. KUSA-A1 cultured in medium supplemented with beta-glycerophosphate was stained in situ by the von Kossa technique. Discrete mineralized nodules are seen. (B) Transmission electron micrograph (TEM) of a nodule present in a KUSA-A1 culture 14 days post-confluence. The extracellular matrix produced by KUSA-A1 cells was observed on the cell surface [arrow]. (C) High-power view of panel B. TEM revealed that the sphere of extracellular matrix produced by KUSA-A1 cells contained a small granular material [arrowhead]. (D) High-power view of a KUSA-A1 cell. Many lysosomal myelin-like figures [arrow] and rough endoplasmic reticulum are seen in its cytoplasm. (E) High-power view of KUSA-A1 cells. Abundant collagen fibrils are visible in the intercellular spaces [arrow], and the cytoplasm contains rough endoplasmic reticulum. Scale bars: 1 mm (A), 20 μm (B), 5 μm (C, D), and 1 μm (E).

observed on the cell surface (Fig. 3C). The cytoplasm of the spindle-shaped cells contained extensive, dilated, and rough endoplasmic reticulum and myelin-like lysosomes (Fig. 3D). Lysosome-rich cells were found in the bone nodules. These cells are probably similar to those observed in vivo [16] and in the primary bone cell cultures [17]. The cells produce abundant, orthogonally oriented collagen fibrils in the intercellular spaces (Fig. 3E), and these fibrils were also found in membrane folds.

3.3. Gap-junctional communication in KUSA-A1 cells

Gap-junctional communication is required for the osteoblast maturation process in culture [18,19], and we used the dye-transfer method to assess the gap-junctional communication between KUSA-A1 cells. When Fluorescent Lucifer Yellow CH was injected into a KUSA-A1 cell, the dye was rapidly transferred to the neighboring cells (Fig. 4A and B), implying that KUSA-A1 cells constitutively communicate with each other via gap junctions.

The expression of gap-junction genes by KUSA cells was investigated by blot hybridization of stromal cell RNA with a connexin 43 cDNA probe. H-1/A of the marrow preadipocyte cell line is a positive control. Distinct 3.0-kb mRNA bands were observed in all of the marrow stromal cell lines when tested with the connexin 43 cDNA probe (Fig. 4C), but no bands were detected in any of the cells when tested with a connexin 32 probe (data not shown).

3.4. Microscopic examination of large subcutaneous masses

NIH3T3, KUM3, KUM4, and KUSA cells transfected with MTAg were designated NIH3T3-MTAg, KUM3-MTAg, KUM4-MTAg, and KUSA-MTAg cells, respectively. Four weeks after subcutaneous inoculation of 10^7 NIH3T3-MTAg, KUM3-MTAg, KUM4-MTAg, KUSA-MTAg, and untransfected KUSA-A1 cells [6] into immunodeficient mice, masses had formed in the subcutaneous tissue. The masses were of three types histologically. Sarcoma-type masses were induced by NIH3T3-MTAg, KUM3-MTAg, and KUM4-MTAg cells and diagnosed as fibrocytic sarcoma; they did not contain bone. The tumors consisted of pleomorphic mesenchymal cells, including multinucleated bizarre giant cells (Fig. 5A and B). The second type of masses was sarcomas with complete bone formation. KUSA-MTAg cells induced sarcomas, most of which contained well-defined complete bone. These sarcomas exhibited an irregular woven pattern of pleomorphic spindle cells that included multinucleated tumor giant cells (Fig. 5C–E). The third type of masses consisted of complete bone and bone cavities with trilineage hematopoiesis. Untransfected KUSA cells formed bone (Fig. 5F–H). Untransfected KUSA-A1 cells, a subclone of the KUSA cells, also formed complete bone 4 weeks after inoculation (Fig. 5I and J). No sarcomatous cell proliferation was observed.

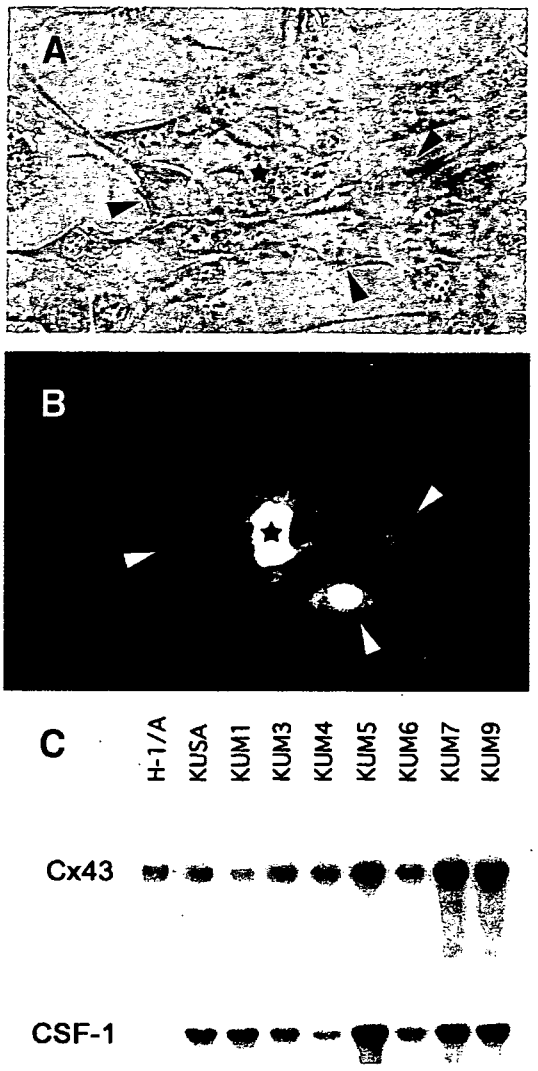

Fig. 4. Dye transfer in KUSA-A1 cells at semiconfluence. Intercellular communication was assessed by the dye transfer method. A and B: Phase-contrast micrograph (A) and fluorescence photograph (B) of KUSA-A1 cells. A KUSA-A1 cell [asterisk] was injected with Lucifer Yellow CH, and the dye was transferred to several adjacent cells. The dye has spread to three first-order-neighboring cells [arrowheads]. (C) Analysis of connexin 43 (Cx. 43) expression by KUSA, KUM1, KUM3, KUM4, KUM5, KUM6, KUM7, and KUM9 cells at semiconfluence. The same blot, which was rehybridized with the CSF-1, is shown for reference [6] in the lower panel.

3.5. Ossification by KUSA-A1 is membranous

To determine whether the ossification by KUSA-A1 is membranous or enchondral, we followed the time-course of KUSA-A1 ossification in the subcutaneous tissue of SCID mice after injecting cells 7 days post-confluence. The injected cells had produced a meshwork of collagen fibers and amorphous ground substance (osteoid matrix) at 1 week (Fig. 6A), and the fibers and ground substance markedly increased and became larger. The matrix was highly calcified at 4 weeks (Fig. 6B and C), and marrow cavities had formed inside the KUSA-A1 bone.

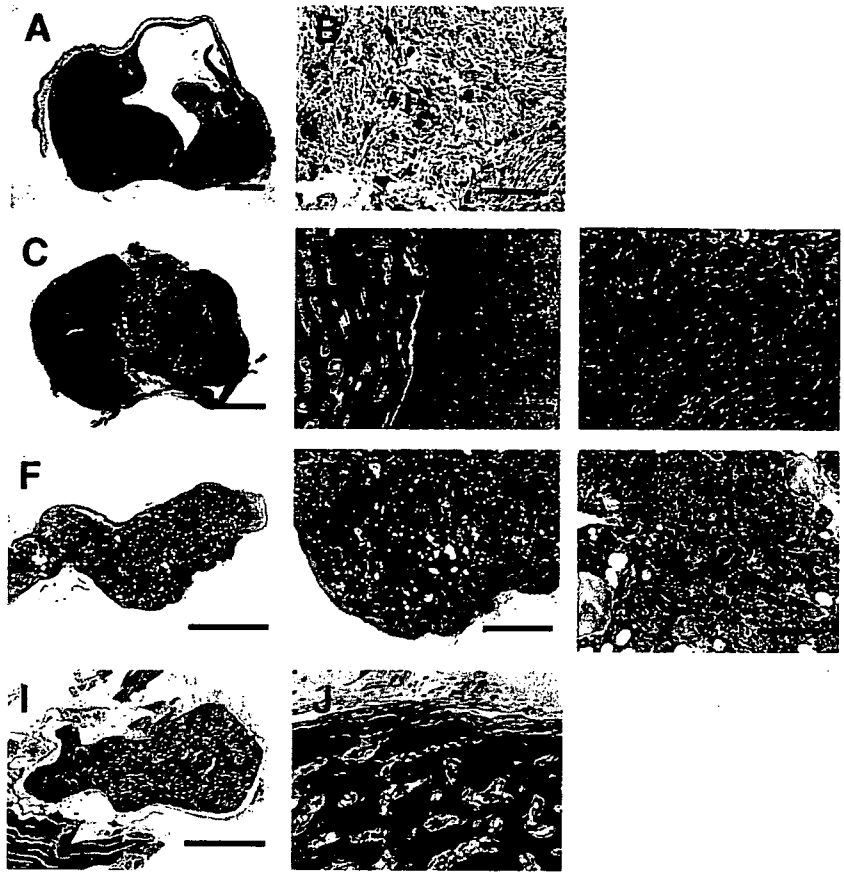

Fig. 5. Microscopic appearance of subcutaneous masses 4 weeks after subcutaneous inoculation of NIH3T3-MTAg (A, B), KUSA-MTAg (C, D, E), KUSA (F, G, H), and KUSA-A1 cells (I, J). (A) Mass of the first type. It is a sarcoma [s] without bone. (B) High-power view of a part of panel (A). The tumor consists of pleomorphic mesenchymal cells, including multinucleated bizarre giant cells. (C, D) Mass of the second type. The mass is composed of sarcoma [s] and well-defined bone [b]. (E) High-power view of part of the tumor in panel (D). The tumor shows proliferation of pleomorphic spindle cells, including giant multinucleated tumor cells. (F, G) Mass of the third type. The mass is composed of complete bone with bone cavities [asterisks], but there is no sarcomatous proliferation. (H) High-power view of part of the mass in panel (G). Trilineage hematopoietic cells (granulocytes [g], erythrocytes [e], and megakaryocyte [arrow]) in the bone cavities inside the mass are shown. (I) Mass of the third type. The mass is composed of complete bone with bone cavities [asterisks], but there is sarcomatous proliferation. (J) High-power view of panel (I). H–E stain. Scale bars: 2 mm (A, C, F, K), 0.5 mm (G), 200 μm (D), and 100 μm (B, E, H, J).

Histological examination of complete bone mass revealed highly dense bone trabeculae, and hematopoietic cells were observed in the bone marrow, as reported previously [6,10]. No cartilage had formed in any of the KUSA-A1-produced bones, indicating that the osteogenesis by KUSA-A1 is membranous ossification rather than enchondral ossification. Osteogenesis was monitored radiographically at scheduled times after the inoculation of $3-5 \times 10^7$ KUSA-A1 cells, and the results showed a gradual increase in newly formed bone 2 weeks after the injection, and complete bone density 4 weeks after the inoculation.

We then monitored the fate of KUSA-A1 bone transplanted into subcutaneous tissue and the abdominal cavity and found that the ectopic KUSA-A1 bone remained unchanged in size and shape for 12 months at both sites. Histological examination revealed complete functional hematopoiesis by ectopic KUSA-A1 bone in the subcutaneous tissue, but not in the abdominal cavity.

Fig. 6. The process of osteogenesis by KUSA-A1 cells in vivo. (A) One week after the inoculation of 10^7 KUSA-A1 cells, bone formation [arrows] was observed around the periphery of the mass at all inoculation sites. It is noteworthy that no chondrogenesis was observed during early osteogenesis. (B) Two weeks after inoculation. There is more bone matrix [arrows] at week 2 than at week 1. (C) Four weeks after inoculation, the mass consists of complete bone tissue [b] and bone cavities [asterisks]. H–E stain. Scale bars: 100 μm.

4. Discussion

4.1. KUSA-A1 cells can be used as a model for developmental bone formation and abnormal ossification

The sequence of KUSA-A1 bone formation is as follows: deposition of matrix by KUSA-A1 cells that subsequently become mineralized, deposition of bone as a network of immature or woven trabeculae, and formation of bone marrow or conversion of the spongiosa into primary cortical bone by filling of spaces between the trabeculae. This process results in the formation of cancellous bone and bone marrow. Importantly, the osteogenesis by KUSA-A1 cells was irreversible and reproducible, and the transplanted KUSA-A1 cells never transformed into malignant cells, formed any abnormal extracellular matrices, or induced any significant inflammatory reactions. It is noteworthy that the osteogenesis by KUSA-A1 cells was not mediated by chondrogenesis, and it was therefore considered to be membranous ossification. Thus, the unique characteristics of KUSA-A1 cells provide an opportunity to analyze the process of membranous ossification in an experimental system in detail.

In fetal life, primary ossification centers form by one of two processes: endochondral ossification or membranous ossification. Endochondral ossification refers to bony replacement of cartilage and is the mode of formation of the long bones. During membranous ossification, mesenchymal cells form membranes within which ossification occurs, and this is the mode of formation of the scapula and skull and, in part, of the clavicle and pelvis. After birth, bone growth continues by both endochondral and membranous ossification. Further endochondral ossification occurs in the physes and results in continuous longitudinal growth of the long bones until skeletal maturity. KUSA-A1 cells were obtained from a long bone the femur, but formed bone by membranous ossification. There are also cells responsible for the periosteal membranous ossification in tubular bones, which model the diaphyseal cortex, and KUSA-A1 cells may be derived from such a minor cell population in long bones that is responsible for periosteal bone formation or callus.

The process of ossification by KUSA-A1 cells may also serve a model for ectopic or heterotopic ossification, such as soft tissue ossification, ligament ossification, and heterotopic bone formation in a number of disorders, including central nervous system and spinal cord disorders, probably as a consequence of immobilization, a model of myositis ossificans progressiva, which often develops after a traumatic event, and a model of ossification of the posterior longitudinal ligament of the spine, which is characterized by the presence of a linear band of ossification along the posterior margin of vertebral bodies and intervertebral discs, especially in the cervical spine.

4.2. Possibility of implanted-cell transformation

The lack of tumor formation or in vivo transformation after implantation of KUSA-A1 cells into immunodeficient mice does not mean that the donor cells are incapable of transforming after implantation, at least in mice. The observation period after cell implantation into mice is usually less than 1 year because the life span of mice is approximately 2 years. By contrast, since patients who receive cell-based therapy may survive for decades, the possibility of implanted-cell transformation cannot be ignored. Care should be exercised when using donor cells transfected with certain genes for the therapeutic purposes, because zero risk of implanted-cell transformation cannot be achieved, even though human non-tumor cells seldom transform in vitro or in vivo without gene transfection.

4.3. Can cancellous bone grafting be replaced by osteoblast-based therapy?

The transplantation of bone from one site to another usually promotes osteogenesis or provides structural stability. Grafts may be used to fill bone defects, promote union, or provide material for arthrodesis. The donor sites most frequently used for grafts are the iliac crest, tibia, and fibula. Depending on circumstances, the patient or animal may receive either a cancellous bone graft or a cortico-cancellous graft. Cancellous bone grafts are the gold standard for bone defects. They have greater capacity to induce new bone formation and, thus, are considered to be generally much more successful in inducing new bone formation than osteoblast-based therapy. Osteoblast-based therapy is poorer than cancellous bone grafts in providing structural stability.

However, complications occur after cancellous bone grafting and include fracture at the donor site, intraoperative bleeding, and postoperative pain. Graft failure may lead to progressive bone resorption and, ultimately, to disappearance of the graft. Follow-up radiographs show healing of iliac donor sites with sclerosis at the margins of the bone defects. Painful excrescences of the bone may develop at the donor site. Loss of the sharp margins between the graft and host bone on radiographs generally signifies graft healing, and the persistence of a thin residual radiolucent area between the graft and the host bone suggests fibrous union.

It would be interesting to assess the possibility of using mature osteoblasts as a therapeutic agent. The inoculation of isolated mature osteoblasts into a bone defect or fracture site would be a more efficient means of accelerating bone fusion with minimal invasion than inoculation of unfractionated marrow cells into fracture sites. The critical step in realizing osteoblast-based therapy will be the isolation of human counterparts to KUSA-A1 cells and growing them in sufficient numbers in culture. The separation of osteoblasts from human marrow stroma [21] and inoculation of the cells with an appropriate scaffold will provide new methods of

osteogenesis engineering without any of the complications associated with cancellous bone grafts.

Acknowledgements

We would like to express our sincere thanks to Y. Takeda and H. Abe for support throughout the work, and to N. Hida, T. Inomata, Y. Hashimoto, and Y. Nakamura, for providing expert technical assistance. This study was supported by a grant from the Ministry of Education, Culture, Sports, Science, and Technology of Japan, the Health and Labour Sciences Research Grants, and the Pharmaceuticals and Medical Devices Agency to A. U.

References

[1] P. Bianco, P.G. Robey, Marrow stromal stem cells, J. Clin. Invest. 105 (2000) 1663–1668.
[2] M.C. Horowitz, A. Fields, D. DeMeo, H.Y. Qian, A.L. Bothwell, E. Trepman, Expression and regulation of Ly-6 differentiation antigens by murine osteoblasts, Endocrinology 135 (1994) 1032–1043.
[3] E. Canalis, Novel treatments for osteoporosis, J. Clin. Invest. 106 (2000) 177–179.
[4] G.A. Rodan, T.J. Martin, Therapeutic approaches to bone diseases, Science 289 (2000) 1508–1514.
[5] M.F. Pittenger, A.M. Mackay, S.C. Beck, R.K. Jaiswal, R. Douglas, J.D. Mosca, M.A. Moorman, D.W. Simonetti, S. Craig, D.R. Marshak, Multilineage potential of adult human mesenchymal stem cells, Science 284 (1999) 143–147.
[6] A. Umezawa, T. Maruyama, K. Segawa, R.K. Shadduck, A. Waheed, J. Hata, Multipotent marrow stromal cell line is able to induce hematopoiesis in vivo, J. Cell. Physiol. 151 (1992) 197–205.
[7] S. Makino, K. Fukuda, S. Miyoshi, F. Konishi, H. Kodama, J. Pan, M. Sano, T. Takahashi, S. Hori, H. Abe, J. Hata, A. Umezawa, S. Ogawa, Cardiomyocytes can be generated from marrow stromal cells in vitro, J. Clin. Invest. 103 (1999) 697–705.
[8] S. Gojo, N. Gojo, Y. Takeda, T. Mori, H. Abe, S. Kyo, J. Hata, A. Umezawa, In vivo cardiovasculogenesis by direct injection of isolated adult mesenchymal stem cells, Exp. Cell Res. 288 (2003) 51–59.
[9] J. Kohyama, H. Abe, T. Shimazaki, A. Koizumi, K. Kashima, S. Gojo, T. Taga, H. Okano, J. Hata, A. Umezawa, Brain from bone: efficient 'meta-differentiation' of marrow stroma-derived mature osteoblasts to neurons with Noggin or a demethylating agent, Differentiation 68 (2001) 235–244.
[10] K. Ochi, G. Chen, T. Ushida, S. Gojo, K. Segawa, H. Tai, K. Ueno, H. Ohkawa, T. Mori, A. Yamaguchi, Y. Toyama, J. Hata, A. Umezawa, Use of isolated mature osteoblasts in abundance acts as desired-shaped bone regeneration in combination with a modified poly-DL-lactic-co-glycolic acid (PLGA)-collagen sponge, J. Cell. Physiol. 194 (2003) 45–53.
[11] A. Sharov, et al., Transcriptome analysis of mouse stem cells and early embryos, PLoS Biol. 1 (2003) E74.
[12] A. Umezawa, K. Harigaya, H. Abe, Y. Watanabe, Gap-junctional communication of bone marrow stromal cells is resistant to irradiation in vitro, Exp. Hematol. 18 (1990) 1002–1007.
[13] A. Umezawa, J. Hata, Expression of gap-junctional protein (connexin 43 or alpha 1 gap junction) is down-regulated at the transcriptional level during adipocyte differentiation of H-1/A marrow stromal cells, Cell Struct. Funct. 17 (1992) 177–184.
[14] A. Umezawa, K. Tachibana, K. Harigaya, S. Kusakari, S. Kato, Y. Watanabe, T. Takano, Colony-stimulating factor 1 expression is down-regulated during the adipocyte differentiation of H-1/A marrow stromal cells and induced by cachectin/tumor necrosis factor, Mol. Cell. Biol. 11 (1991) 920–927.
[15] H. Sudo, A. Kodama, Y. Amagai, S. Yamamoto, S. Kasai, In vitro differentiation and calcification in a new clonal osteogenic cell line derived from newborn mouse calvaria, J. Cell Biol. 96 (1983) 191–198.
[16] S.B. Doty, B.H. Schofield, Enzyme histochemistry of bone and cartilage cells, Prog. Histochem. Cytochem. 8 (1976) 1–38.
[17] I. Binderman, D. Duksin, A. Harell, E. Katzir, L. Sachs, Formation of bone tissue in culture from isolated bone cells, J. Cell Biol. 61 (1974) 427–439.
[18] P.C. Schiller, G. D'Ippolito, W. Balkan, B.A. Roos, G.A. Howard, Gap-junctional communication is required for the maturation process of osteoblastic cells in culture, Bone 28 (2001) 362–369.
[19] M.M. Saunders, J. You, J.E. Trosko, H. Li, Z. Yamasaki, H.J. Donahue, C.R. Jacobs, Gap junctions and fluid flow response in MC3T3-E1 cells, Am. J. Physiol., Cell Physiol. 281 (2001) C191725.
[20] P.S. Leboy, J.N. Beresford, C. Devlin, M.E. Owen, Dexamethasone induction of osteoblast mRNAs in rat marrow stromal cell cultures, J. Cell. Physiol. 146 (1991) 370–378.
[21] T. Mori, T. Kiyono, H. Imabayashi, Y. Takeda, K. Tsuchiya, S. Miyoshi, H. Makino, H. Matsumoto, H. Saito, S. Ogawa, M. Sakamoto, J-i Hata, A. Umezawa, Combination of hTERT and Bmi-1, E6 or E7 induce prolongation of the life span of bone marrow stromal cells from an elderly donor without affecting their neurogenic potential, Mol. Cell. Biol. 25 (2005) 5183–5195.

MOLECULAR AND CELLULAR BIOLOGY, June 2005, p. 5183–5195 Vol. 25, No. 12
0270-7306/05/$08.00+0 doi:10.1128/MCB.25.12.5183–5195.2005

Combination of hTERT and *bmi-1*, E6, or E7 Induces Prolongation of the Life Span of Bone Marrow Stromal Cells from an Elderly Donor without Affecting Their Neurogenic Potential†

Taisuke Mori,[1,2,3] Tohru Kiyono,[3] Hideaki Imabayashi,[1,4] Yukiji Takeda,[1,2,6] Kohei Tsuchiya,[1] Shunichirou Miyoshi,[5] Hatsune Makino,[1] Kenji Matsumoto,[7] Hirohisa Saito,[7] Satoshi Ogawa,[5] Michiie Sakamoto,[2] Jun-Ichi Hata,[1] and Akihiro Umezawa[1]*

Department of Reproductive Biology and Pathology, National Research Institute for Child Health and Development, Tokyo, Japan[1]; Department of Pathology, Keio University School of Medicine, Tokyo, Japan[2]; Virology Division, National Cancer Center Research Institute, Tokyo, Japan[3]; Department of Orthopedic Surgery, Keio University School of Medicine, Tokyo, Japan[4]; Cardiopulmonary Division, Department of Internal Medicine, Keio University School of Medicine, Tokyo, Japan[5]; Department of General Medicine and Clinical Investigation, Nara Medical University, Nara, Japan[6]; and Department of Allergy and Immunology, National Research Institute for Child Health and Development, Tokyo, Japan[7]

Received 11 January 2005/Returned for modification 13 February 2005/Accepted 14 March 2005

Murine bone marrow stromal cells differentiate not only into mesodermal derivatives, such as osteocytes, chondrocytes, adipocytes, skeletal myocytes, and cardiomyocytes, but also into neuroectodermal cells in vitro. Human bone marrow stromal cells are easy to isolate but difficult to study because of their limited life span. To overcome this problem, we attempted to prolong the life span of bone marrow stromal cells and investigated whether bone marrow stromal cells modified with *bmi-1*, hTERT, E6, and E7 retained their differentiated capability, or multipotency. In this study, we demonstrated that the life span of bone marrow stromal cells derived from a 91-year-old donor could be extended and that the stromal cells with an extended life span differentiated into neuronal cells in vitro. We examined the neuronally differentiated cells morphologically, physiologically, and biologically and compared the gene profiles of undifferentiated and differentiated cells. The neuronally differentiated cells exhibited characteristics similar to those of midbrain neuronal progenitors. Thus, the results of this study support the possible use of autologous-cell graft systems to treat central nervous system diseases in geriatric patients.

Murine and human bone marrow stromal cells differentiate into osteoblasts (2), chondrocytes (13), skeletal myocytes, adipocytes, and cardiomyocytes (24) in vitro and thus are a useful cell source for bone regeneration (26) and in vivo cardiovasculogenesis (11). However, recent studies suggest that bone marrow stromal cells can also differentiate into a neuronal lineage (22), and murine bone marrow-derived multipotent adult progenitor cells differentiate into dopaminergic neuronal cells (16). Since the use of bone marrow stromal cells entails no ethical or immunological problems, and bone marrow aspiration is an established routine procedure, they may be a useful source of cells for transplantation.

Large numbers of cells may be necessary for repairing damaged human tissues to restore function. However, there have been no reports of a sufficient number of differentiated neurons ever having been obtained from human marrow stromal cells. One reason is that normal human cells undergo a limited number of divisions in culture and then enter a nondividing state referred to as "senescence." Senescence is classified into two categories: "stress-induced premature senescence," or "telomere-independent senescence," and "replicative senescence," or "telomere-dependent senescence" (3, 5, 38). $p16^{Ink4a}$ (p16), a cyclin-dependent kinase (CDK) inhibitor, is induced by certain oncogenes and other damage or stress signals and is required for "premature senescence" in human mammary epithelial cells and keratinocytes. p16 inhibits dephosphorylation of pRb by Cdk4/6-cyclin D, and hypophosphorylated pRb actively represses the genes required for the S phase by sequestering the E2F transcription factors. "Replicative senescence" is caused by telomere size reduction during successive cell divisions because of the chromosome end replication problem. Ectopic expression of telomerase alone bypasses replicative senescence in certain cell types, such as human foreskin fibroblasts.

To obtain enough human cells to restore the function of failing organs and to establish a model of cell therapy, the life span of human marrow stromal cells was extended by infecting them with retrovirus encoding human telomerase reverse transcriptase (hTERT) and the human papillomavirus E6 and E7 genes. Both p16/Rb inactivation by E7 and telomerase activation by E6 are required to extend the life span of human

* Corresponding author. Mailing address: Department of Reproductive Biology and Pathology, National Research Institute for Child Health and Development, 2-10-1 Okura, Setagaya-ku, Tokyo 157-8535, Japan. Phone: 81-3-5494-7047. Fax: 81-3-5494-7048. E-mail: umezawa@1985.jukuin.keio.ac.jp.

† Supplemental material for this article may be found at http://mcb.asm.org/.

mammary epithelial cells (21) and umbilical cord blood-derived cells (36). E6 also accelerates the degradation of p53, which induces the CDK inhibitor p21 (35). In contrast to foreskin fibroblasts (5), however, the increase in telomerase activity as a result of the introduction of hTERT is insufficient to prolong the life span of marrow stromal cells (27).

The protocols for in vitro differentiation into neuronal cells include the use of a demethylating agent and/or the neurotrophic cytokines, such as nerve growth factor (NGF), brain-derived neurotrophic factor (BDNF), and neurotrophin 3. Basic fibroblast growth factor (bFGF) activates essential neuronal transcription factors, such as Hes-1 (10), in neural precursor cells and embryonic stem cells (19, 31). The Notch-Hes1 pathway plays an essential role in inhibition of neuronal differentiation (17), and the B27 supplement is effective in achieving long-term viability of primary neurons in culture (7). Taking these findings into consideration, a simple protocol for neural transdifferentiation was developed in this study.

The first purpose of this study was to determine whether prolonging the cell life span with cell cycle-associated molecules would inhibit neurogenic differentiation of marrow stromal cells in vitro. The second purpose was to determine if transdifferentiation of marrow cells of mesodermal origin to neurogenic cells was accompanied by global changes in gene expression or only leaky expression of some neurogenic markers. The in vitro differentiation process appears to be highly specific, and the life span of marrow-derived stromal cells can be extended by retrovirus-mediated transfer of the *bmi-1* gene, which reduces expression of p16 (14, 15, 37), stimulates cell proliferation (9), and is required for maintenance of self-renewing hematopoietic stem cells (29).

MATERIALS AND METHODS

Isolation and cell culture. After signed informed consent was obtained, bone marrow cells were harvested from a 91-year-old human female donor with the approval (approval numbers 13-1 and 12-1) of the Ethics Committee of Keio University School of Medicine. The cells were resuspended in growth medium (MSCGM, PT-3238, and PT-4105; Cambrex Bio Science Walkersville, Inc., Walkersville, MD) and cultured as previously described (1, 13). Several bone marrow stromal cell strains, designated H4-1, H4-2, and H4-3, were generated from primary or first-passage cells using the limiting dilution method. The cells were cultured for further experiments under the approval (approval numbers 25 and 49) of the Ethics Committee of the National Research Institute for Child Health and Development, Tokyo, Japan.

Infection with recombinant retroviruses. The cells were prepared for infection with recombinant retroviruses carrying the *bmi-1*, E6, E7, and hTERT genes, as previously described (1). Stably transduced cells with an expanded life span were designated UBT-5, UBE6T-6, UBE6T-7, UE7T-9, UE6E7T-11, UE6E7T-12, UE7T-13, UBT-15, and UE6E7-16 cells.

Neuronal differentiation of bone marrow stromal cells. Cells removed from the flask bottom were replated onto a coverslip coated with laminin-polylysine (no. 354455; Becton Dickinson BioScience) in MSCGM. One day after passage, the medium was replaced with B27-supplemented Dulbecco's modified Eagle's medium-F12 (Gibco, BRL) containing 20 ng/ml of BDNF (R&D), 10 ng/ml of bFGF (R&D), and 50 ng/ml of NGF (Invitrogen) for neuroectodermal differentiation. Bone marrow stem cells were processed for immunocytochemistry and reverse transcription (RT)-PCR 7 to 21 days after induction.

RT-PCR. Total RNA was prepared from cultured cells with Isogen (Nippon Gene, Tokyo, Japan). Human neuronal RNA was purchased (human total brain RNA; lot 2110667; Becton Dickinson BioScience). RNA for RT-PCR was converted to cDNA with a First-strand cDNA Synthesis kit (Amersham Pharmacia Biotech) according to the manufacturer's recommendations. The following PCR primer sets were used for neuron-associated genes: nestin mRNA, sense (5′-AGAGGGGAATTCCTGGAG-3′) and antisense (5′-CTGAGGACCAGGACTCTCTA-3′); NF-M mRNA, sense (5′-TGAGCTACACGTTGGACTCG-3′) and antisense (5′-TCTCCGCCTCAATCTCCTTA-3′); notch-I mRNA, sense (5′-TCACGCTGACGGAGTACAAG-3′) and antisense (5′-CCACACTCGTTGACATCCTG-3′); Sox-2 mRNA, sense (5′-CACAACTCGGAGATCAGCAA-3′) and antisense (5′-GTTCATGTGCGCGTAACTGT-3′); neuronal cell adhesive molecule (N-CAM) mRNA, sense (5′-TCCATCACCTGGAGGACTTC-3′) and antisense (5′-CTCCAGATAGCTGGCAGAGG-3′); MAP-2 mRNA, sense (5′-GGATTCTGGCAGCAGTTCTC-3′) and antisense (5′-TCCTTGCAGACACCTCCTCT-3′); tubulin-beta III mRNA, sense (5′-ACCTCAACCACCTGGTATCG-3′) and antisense (5′-TGCTGTTCTTGCTCTGGATG-3′); and Nur-related factor-1 (Nurr1) mRNA, sense (5′-TTTCTGCCTTCTCCTGCATT-3′) and antisense (5′-GTGGCACCAAGTCTTCCAA-3′); 18S mRNA sense (5′-GTGGAGCGATTTGTCTGGTT-3′) and antisense (5′-CGCTGAGCCAGTCAGTGTAG-3′) were used as a positive control. PCR was performed with TaKaRa Z-Taq (TAKARA SHUZO Co., Ltd.) for 30 cycles, with each cycle consisting of 98°C for 5 s, 68°C or 60°C for 1 s, and 72°C for 10 s, with an additional 30-s incubation at 72°C after completion of the final cycle.

Western blot analysis. To detect p16, p53, p21, p27, Rb, Bmi-1, and actin, immunoblotting was performed as previously described (30) with antibodies against p16 (G3-245; BD Pharmingen, San Diego, CA), Rb (G174-405; BD Pharmingen), p53 (DO-1), p21 (Ab-1; Oncogene Science, Boston, MA), Bmi-1 (monoclonal antibody generated by T. Kiyono), p27 (BD Pharmingen), and actin (Santa Cruz Biotechnology Inc., Santa Cruz, CA).

Telomere length assay. Genomic DNA was extracted from cultured cells. Restriction enzyme digestion of genomic DNA was carried out with HinfI and RsaI. The fragments obtained were resolved on 0.7% agarose gels, transferred to a Hybond N membrane (Amersham, United Kingdom), and hybridized with digoxigenin-labeled $(TTAGGG)_3$ probe. The membrane was then incubated with anti-digoxigenin alkaline phosphatase, and detection was performed with a chemiluminescence solution. The size range and intensity were determined with X-ray film.

Telomerase activity analysis. Telomerase activity was determined with a telomere repeat amplification protocol (TRAP) assay kit, Telo TAGGG telomerase PCR ELISA plus (Roche, Indianapolis, IN), according to the manufacturer's instructions.

G-banding karyotypic analysis. Metaphase spreads were prepared from cells treated with Colcemid (Karyo Max; Gibco BRL; 100 ng/ml for 6 h). We performed a standard G-banding karyotypic analysis on at least 50 metaphase spreads for each population.

SKY analysis. Spectral karyotyping (SKY) was performed on metaphase-transduced cells (UBE6T-7, UE6E7T12, and UE7T13) in 80 population doublings (PDs) according to the kit manufacturer's instructions (ASI, Carlsbad, CA) and a previously published method (34).

Immunocytochemical analysis. Immunocytochemical analysis was performed as previously described (30) with antibodies to MAP-2 (Zymed, San Francisco, CA), tubulin 3 (Sigma, St. Louis, Missouri), GFAP (DAKO, Denmark), Nurr1 (N-20; Santa Cruz), and nestin (Biogenesis, United Kingdom) in phosphate-buffered saline containing 1% bovine serum albumin. As a methodological control, the primary antibody was omitted. After being washed in phosphate-buffered saline, the slides were incubated with fluorescein isothiocyanate-conjugated anti-mouse immunoglobulin antibody or phycoerythrin (PE)-conjugated anti-rabbit immunoglobulin antibody (DAKO, Denmark).

GeneChip expression analysis. Human genomewide gene expression was examined with the Human Genome U133A Probe array (GeneChip; Affymetrix), which contains the oligonucleotide probe set for approximately 23,000 full-length genes and expressed sequence tags, according to the manufacturer's protocol (Expression Analysis technical manual and GeneChip Small Sample Target Labeling Assay version 2 technical note [http://www.affymetrix.com/support/technical/index.affx]). Total RNA was isolated with an RNeasy minikit (QIAGEN, Chatsworth, CA). Double-stranded cDNA was synthesized, and the cDNA was subjected to in vitro transcription in the presence of biotinylated nucleoside triphosphates. The biotinylated cRNA was hybridized with a probe array for 16 h at 45°C, and the hybridized biotinylated cRNA was stained with streptavidin-PE and scanned with a Hewlett-Packard Gene Array Scanner. The fluorescence intensity of each probe was quantified by using the GeneChip Analysis Suite 5.0 computer program (Affymetrix). The expression level of a single mRNA was determined as the average fluorescence intensity among the intensities obtained with 11 paired (perfectly matched and single-nucleotide-mismatched) probes consisting of 25-mer oligonucleotides. If the intensities of mismatched probes were very high, gene expression was judged to be absent, even if high average fluorescence was obtained with the GeneChip Analysis Suite 5.0 program. The level of gene expression was determined with the GeneChip software as the average difference (AD). Specific AD levels were then calculated as percentages of the mean AD level of six probe sets for housekeeping genes (actin and GAPDH [glyceralde-

hyde-3-phosphate dehydrogenase] genes). Further data analysis was performed with Genespring software version 5 (Silicon Genetics, San Carlos, CA). To normalize the staining intensity variations among chips, the AD values for all genes on a given chip were divided by the median of all measurements on that chip. To eliminate changes within the range of background noise and to select the most differentially expressed genes, data were used only if the raw data values were less than 100 AD and gene expression was judged to be present by the Affymetrix data analysis. Hierarchical clustering analysis with standard correlation was used to identify gene clusters. The separation ratio was set at 0.5. Normalization values were considered significant when (i) expression changed by at least twofold (activation program) and (ii) increased gene expression included at least one present absolute call (Affymetrix algorithm). Normalized values were averaged for two donors and used for the data analysis, and the normalized values were used to classify the genes into up-regulated or down-regulated. There was a statistically significant correlation between the expression levels of genes of the same cells analyzed twice ($r = 0.997$). These criteria confirmed the reproducibility of the differences that were seen between different cells under different conditions.

Calcium imaging. The intracellular Ca^{2+} concentration was monitored by means of the fluorescent Ca^{2+} indicator Fluo-3. The cultured cells were exposed to 10 μmol/liter Fluo-3 acetoxymethylester (Molecular Probes, Eugene, Oregon) at 37°C for 30 min and then washed in Tyrode's solution containing (in mmol/liter) NaCl, 140; KCl, 4; $MgCl_2$, 0.5; $CaCl_2$, 1.8; HEPES, 5; and D-glucose, 55 (pH adjusted to 7.4 with NaOH). The signal from the cell was monitored with a fluorescence microscope (BX50WI; Olympus, Tokyo, Japan) and a high-resolution optical mapping system (MiCAM-01; SciMedia Ltd. Tokyo, Japan) at a wavelength of 530 nm and an excitation wavelength of 488 nm. The cells were challenged with a depolarization stimulus in the form of high-potassium (144 mmol/liter) Tyrode's solution (KCl substituted for NaCl) applied with a rapid solution changer (RSC-160; Molecular Kinetics, Indianapolis, Indiana) at a flow rate of 100 μl/s at a distance of 1 mm from the cell at a room temperature of 25°C. The image analysis was performed with Igor Pro software (Wavemetrics, Lake Oswego, OR) and by customized procedures. The background fluorescence intensity was subtracted from the data, and the areas were normalized to the control response to normal Tyrode's solution and shown on a color scale.

Quantitative RT-PCR. RNA was extracted from cells using the RNeasy kit (QIAGEN, Valencia, CA). Contaminating DNA was eliminated by two sequential DNase (Invitrogen) treatments. An aliquot (1 μg) of total RNA was reverse transcribed by using an oligo(dT) primer. For the thermal cycle reactions, cDNA was amplified (ABI PRISM 7000; Perkin-Elmer Applied Biosystems) using the SYBR RT-PCR kit (Takara Bio, Japan) under the following reaction conditions: 40 cycles of PCR (95°C for 15 seconds and 60°C for 1 min) after an initial denaturation (95°C for 10 min). The controls consisted of amplifications without reverse transcription and reactions without the addition of a cDNA template. The authenticity and sizes of the PCR products were confirmed using a melting curve analysis (using software provided by Perkin-Elmer) and a gel analysis. mRNA levels were normalized using the GAPDH gene as a housekeeping gene. The following primer sets were used: hTERT mRNA, sense (5′-CGGTGTGC ACCAACATCTACAAG-3′) and antisense (5′-TCAGAGATGACGCGCAGG A-3′); Bmi-1 mRNA, sense (5′-CGCTTGGCTCGCATTC-3′) and antisense (5′-AGCTCAGTGATCTTGATTCTCGTTG-3′); E6 mRNA, sense (5′-GCACAG AGCTGCAAACAACT-3′) and antisense (5′-CTCACGTCGCAGTAACTGTT G-3′); E7 mRNA, sense (5′-ATGACAGCTCAGAGGAGGAG-3′) and antisense (5′-TCCTAGTGTGCCCATTAACAG-3′); NR4A2/Nurr1 mRNA, sense (5′-TTCGGCAGAGTTGAATGAATG-3′) and antisense (5′-GAAATTAAAG GTGGACAGTGTCGTA-3′); and GAPDH mRNA, sense (5′-CCAGCCGAG CCACATCGCTC-3′) and antisense (5′-ATGAGCCCCAGCCTTCTCCAT-3′).

Nucleotide sequence accession numbers. The gene chip datasets have been deposited in the GEO database with accession number GSE2110 (GSM38114 to GSM38116).

RESULTS

Human marrow stromal cells with an extended life span. Bone marrow stromal cells were obtained from a 91-year-old human donor and subcloned by limiting dilution. One subclone of the cells isolated was designated H4-1 cells (Fig. 1). To extend the life span of the H4-1 cells and obtain a large number of cells, five different types of cells were obtained by transducing them with combinations of *bmi-1*, E6, E7, and/or TERT genes (http://1985.jukuin.keio.ac.jp/umezawa/cells/name.html). We referred to the cells transduced with *bmi-1* and TERT as UBT-5 and UBT-15 cells, the cells transduced with *bmi-1*, E6, and TERT as UBE6T-6 and UBE6T-7 cells, the cells transduced with E7 and TERT as UE7T-9 and UE7T-13 cells, the cells transduced with E6, E7, and TERT as UE6E7T-11 and UE6E7T-12 cells, and the cells transduced with E6 and E7 as UE6E7-16 cells. Random amplified polymorphic DNA analysis revealed that the five different types of stable transduced cells (UBT-5, UBE6T-7, UE6E7T-12, UE7T-13, and UE6E7-16) were definitely derived from H4-1 cells (see Fig. S1 in the supplemental material).

The UE6E7T-12, UE6E7T-11, UE7T-9, UE7T-13, UBE6T-6, and UBE6T-7 cells were successfully grown and were shown to have extended life spans (Fig. 1A). The life spans of the UE6E7T-12 and UE7T-13 cells were extended to 200 PDs. The life spans of the UBT-5, UBE6T-7, UE6E7T-11, UE7T-9, and UBE6T-6 cells were extended to 60 PDs. The UBT-5 cells also proliferated for more than 60 PDs and were shown to have an extended life span. However, hTERT alone did not extend the life span (data not shown). Nontransduced parental H4-1 cells reached "senescence" in culture at 44 PDs, and UE6E7-16 cells entered a period of "crisis" in culture at 70 PDs (Fig. 1A and B), implying that E6 and E7 are able to prolong the cell life span but that their prolonging effect is limited. The H4-1 cells exhibited large, flat morphology at 40 PDs, while the other cells were small and spindle shaped (Fig. 1C).

None of the cells exhibited malignant transformation activity: they did not form a focus after confluence in vitro; cells grafted into subcutaneous tissue of immunodeficient mice (nonobese diabetic [NOD]-SCID-interleukin 2 receptor knockout mice) did not form tumors, at least during the observation period (more than 30 days); and the morphologies of all clones remained unchanged for 40 to 200 PDs.

Expression of Bmi-1, Rb, p53, p27, and p21 proteins in transduced cells. The expression of cell cycle-associated proteins was analyzed in cells transduced with the hTERT and *bmi-1*, E6, or E7 genes and in parental H4-1 cells (Fig. 2). Human dermal keratinocytes at senescence (PD 27) served as a control for expression of $p16^{Ink4a}$, hypophosphorylated RB, and p53 proteins at a high level.

Bmi-1 proteins were expressed in the UBT-5 and UBE6T-7 cells, but not in the H4-1, UE6E7-12, and UE7T-13 cells. p16 proteins were down-regulated in the *bmi-1*-overexpressing cells, i.e., UBT-5 and UBE6T-7 cells. p53 and p21 proteins were down-regulated in E6-overexpressing UBE6T-7 and UE6E7T-12 cells. These results are consistent with the hypothesis that p53 is proteolysed via ubiquitination by E6 (33). Hypophosphorylated Rb was down-regulated in E7-overexpressing cells, probably as a result of proteolysis by E7. There was no significant difference in p27 protein levels between any of the cells tested.

Increase in telomerase activity and maintenance of telomere length in cells transduced with the hTERT gene. No telomerase activity was detected by the TRAP assay in the parental H4-1 cells at PDs 20 and 40, but telomerase activity was detected in UBT-5, UBE6T-7, UE6E7T-12, and UE7T-13 cells transduced with the hTERT gene at all of the PDs tested. UE6E7-16 cells not transduced with the hTERT gene did not exhibit any telomerase activity at PDs 40 to 120 (Fig. 3A). Likewise, the telomere length of the parental H4-1 cells decreased with the number of PDs, whereas the telomere length

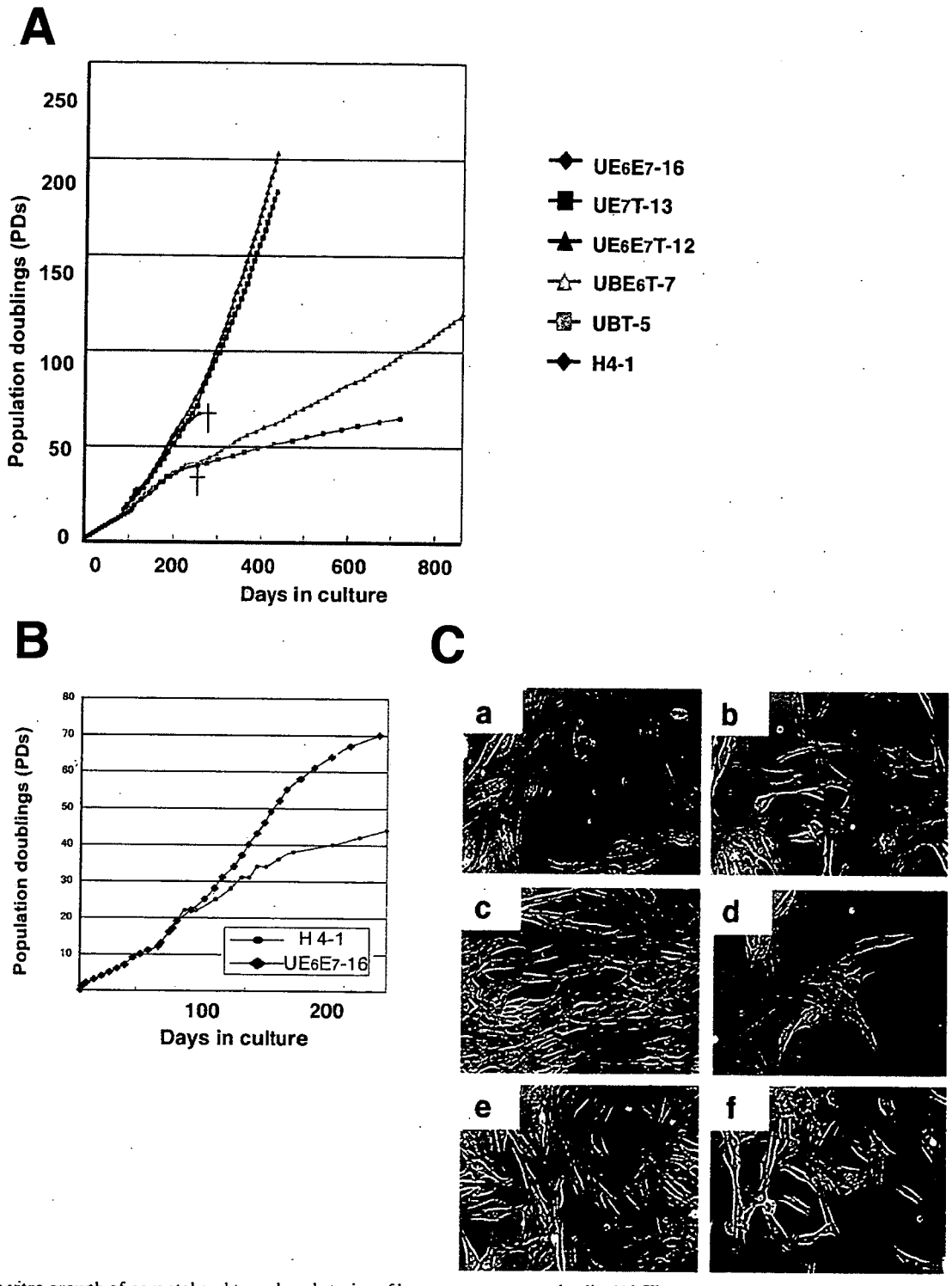

FIG. 1. In vitro growth of parental and transduced strains of bone marrow stromal cells. (A) The population doublings of UE6E7-16, UE7T-13, UE6E7T-12, UBE6T-7, UBT-5, and H4-1 cells are shown. UE7T-13, UE6E7T-12, UBE6T-7, and UBT-5 cells proliferated for over 60 PDs and for more than 400 days. By contrast, parental H4-1 cells and UE6E7-16 cells stopped growing and entered senescence or the growth arrest stage, which is indicated by crosses. (B) H4-1 and UE6E7-16 cells entered senescence at 44 PDs and 70 PDs, respectively, approximately 200 days after the start of culture. (C) Phase-contrast photomicrographs of the bone marrow stromal cells at the semiconfluent stage in a 40-PD culture. (a) H4-1 cells; (b) UBT-5 cells; (c) UBE6T-7 cells; (d) UE6E7T-12 cells; (e) UE7T-13 cells; (f) UE6E7-16 cells.

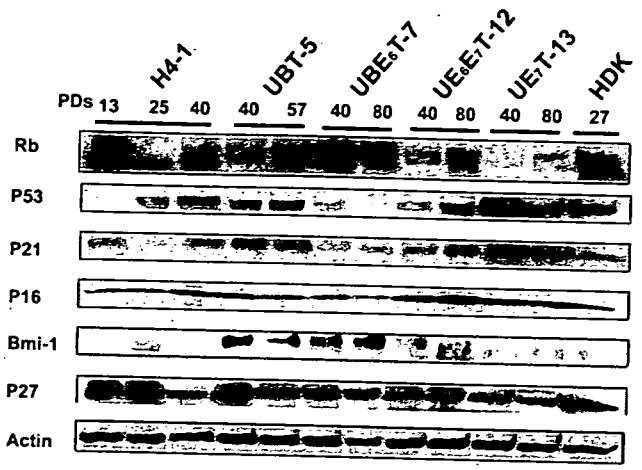

FIG. 2. Time course analysis of cell cycle-associated protein levels in cells with an extended life span. Cell cycle-associated proteins, i.e., Rb, p53, p21, p16, Bmi-1, and p27, in UBT-5, UBE6T-7, UE6E7T-12, UE7T-13, and H4-1 cells were analyzed by Western blotting. Cells cultured for the PDs indicated were assayed. The expression pattern was reproducibly observed in four separate experiments. Expression of actin protein was monitored as a loading control.

of UBT-5, UBE6T-7, UE6E7T-12, and UE7T-13 cells was maintained irrespective of the PD number (Fig. 3B, C, and D).

Karyotypic analysis of parental and transduced cells with extended life spans. We performed a karyotypic analysis (G banding and SKY) of both the parental stromal cells (H4-1) and the cells transduced with hTERT and *bmi-1*, E6, or E7 (see Materials and Methods). SKY permits a detailed analysis of all complex markers and provides insights into their involvement in subsequent rearrangements (34). Our studies raised some interesting points concerning chromosomal abnormality. No genomic abnormalities were found in the parental cells, but an increase in chromosomal number appeared in the other strains, as shown by G-banding and SKY analyses (Table 1 and Fig. 4), except for in the UE7T-13 cells. These abnormalities included translocations, a deletion, other rearrangements, and polyploidy. Surprisingly, we found no genomic changes in the UE7T-13 cells at over 120 PDs.

Establishment of a novel protocol for neuroectodermal differentiation of human marrow stromal cells. Murine stromal cells have been reported to have been transdifferentiated into neuronal lineages (6, 16, 22) by several different protocols. In this study, we devised a simple protocol for neuroectodermal differentiation from mesoderm-derived cells (Fig. 5A). Briefly, growing, adherent stromal cells were trypsinized and pelleted down by centrifugation, and after as much growth medium as possible was aspirated, the pelleted cell aggregates were pipetted with a 20-μl microtip. Each cell aggregate was then replated onto a laminin-coated coverslip in a 7-mm-diameter 24-well culture dish (Fig. 5A), and the growth medium was replaced with B27-supplemented growth medium containing NGF, BDNF, and bFGF. Cells not subjected to this protocol have fibroblast morphology (Fig. 5B, a). The shape of the stromal cells began to change on day 7 after replating, and the cells did not adhere to adjacent cells. The cells then started to exhibit neuron-like morphology that included a refractile round cell body, a neurite-like process(es), and a triangular axon terminal(s) (Fig. 5B, b to d). By days 14 to 21, more than 80% of the bone marrow cells had formed neurite-like processes and exhibited neuron-like morphology. All experiments were repeated at least 10 times using different population doublings (20 to 100 PDs) before using the cells for neuroectoderm differentiation.

Expression of neuron-specific proteins during neuroectodermal differentiation of human marrow stromal cells. After induction, the UBT-5, UBE6T-7, UE6E7T-12, and UE7T-13 cells became positive for the neuron-specific markers microtuble-associated protein 2 (MAP-2), tubulin 3, and Nurr1 (Fig. 5C, a, c, d, k, and n), implying that they could be induced into neuronal lineages. More than 80% of all the tested cells were positive for MAP-2 and Nurr1, but no staining was detected with antibodies against GFAP (an astrocyte-specific marker) or O4 (an oligodendrocyte-specific marker) (data not shown). Undifferentiated UE7T-13 and H4-1 cells did not exhibit neuroectodermal characteristics (Fig. 5C, b and l).

Gene chip analysis during neuroectodermal differentiation. To clarify the specific gene expression profile of human marrow stromal cells, we compared the expression levels of approximately 23,000 genes by neuronally differentiated UE7T-13 cells, undifferentiated UE7T-13 cells, and parental H4-1 cells (GEO accession number GSE2110 [http://1954.jukuin.keio.ac.jp/umezawa/chip/mori]) using the Affymetrix gene chip oligonucleotide arrays. Of the approximately 23,000 genes represented on the gene chip, 2,123 genes were up-regulated to more than twice their expression level in undifferentiated cells. Genes whose expression increased or decreased are shown in Table 2. The Nurr1, kynureninase, apolipoprotein, RARRES1, ABC1, rab27B, STC1, WISP2, rhoGAP6, SLC2A5, and palmderphin genes were among the top 0.1% in terms of increase in expression. Surprisingly, expression of Nurr1/NR4A2, which is essential for differentiation of the nigral dopaminergic neurons (23, 32), was up-regulated 26.1-fold. Wnt-5a promotes the acquisition of dopaminergic neurons (8), and its expression was increased 7.1-fold. These findings imply that the characteristics of these cells are similar to those of midbrain neurons. The dendrogram analysis clearly showed that the change in gene expression pattern is dramatic and neuron specific during neuroectodermal differentiation rather than being leaky, subtle, and nonspecific (Fig. 6).

Expression of neuron-specific genes in differentiated UE7T-13 cells. To confirm the global change in gene expression during neuronal differentiation, RT-PCR was performed with primers that specifically react with human neuronal genes. Differentiated UBT-5, UBE6T-7, UE6E7T-12, UE7T-13, UE6E7-16, and H4-1 cells expressed Nurr1, MAP2, tubulin 3, medium-size neurofilament (NF-M), Sox-2, and nestin, whereas undifferentiated UE7T-13 and H4-1 cells did not express mRNAs for Nurr1, NCAM, nestin, Sox-2, NF-M, or MAP-2 (Fig. 7), implying that these neuron-specific genes began to be expressed in response to the induction protocol (Fig. 5A). Sequence analysis confirmed that the PCR products matched the sequences of the human Nurr1, MAP2, tubulin 3, NF-M, NCAM, Notch-1, Sox-2, and nestin genes. Total brain mRNA was used as a positive control, and expression of all of the genes examined except the nestin gene was observed. The Notch-1 gene, a stem cell-related gene (18), is expressed only in undifferentiated cells and is absent in differentiated cells.

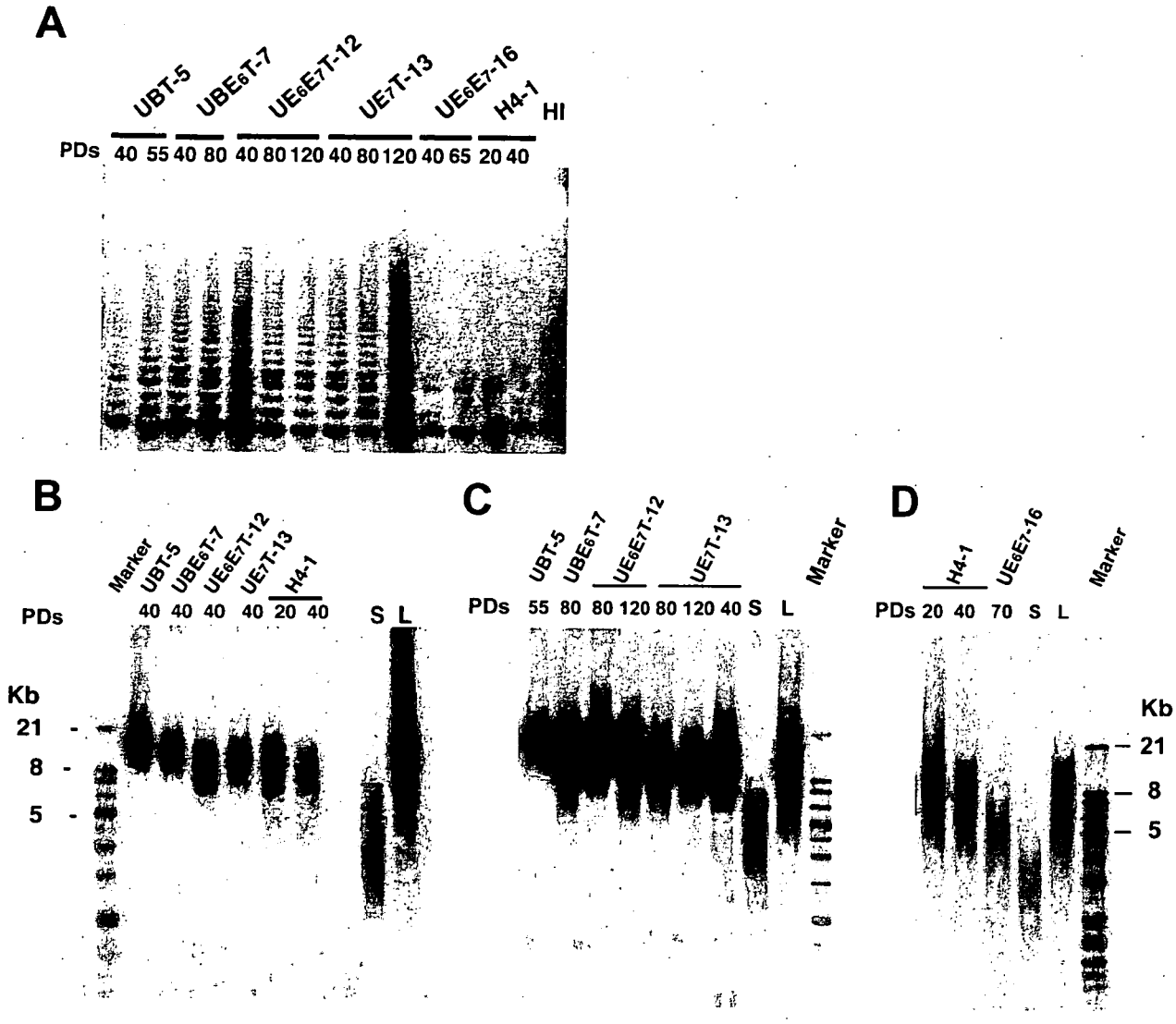

FIG. 3. Telomere activities and telomere lengths of the marrow stromal cells transduced with the hTERT and Bmi-1, E6, or E7 genes. (A) Analysis of telomerase activity by PCR assay in UBT-5, UBE6T-7, UE6E7T-12, UE7T-13, UE6E7-16, and H4-1 cells. Telomerase activity is revealed by the characteristic 6-bp ladder of bands. Heat-inactivated cell lysate (HI) was used as a negative control. (B, C, and D) The mean telomere length of the parental and transduced cells was determined at an early stage (B: 20 to 40 PDs) in UBT-5, UBE6T-7, UE6E7T-12, UE7T-13, and H4-1 cells; a late stage (C: 55 to 120 PDs) in UBT-5, UBE6T-7, UE6E7T-12, and UE7T-13 cells; and a senescent stage (D) in H4-1 and UE6E7-16 cells.

Tubulin 3 was detected at low levels in both differentiated and undifferentiated UE7T-13 cells.

Rapid and reversible calcium uptake by UE7T-13 cells in response to depolarizing stimuli. To determine if the neuronal cells derived from UE7T-13 cells are functional, we exposed the cells to depolarizing stimuli and performed calcium imaging analysis. Cells that had a dendrite component and a smooth-surfaced bright round soma body were selected as the targets for calcium-imaging analysis. Rapid and reversible calcium uptake was observed in neuronally differentiated UE7T-13 cells in response to the change in extracellular potassium concentration (Fig. 8), suggesting that the approximately 20% of the cells that showed uptake have both deep resting membrane potentials and voltage-gated Ca^{2+} channels. The rapid change in extracellular fluid did not cause any stretch-activated channels.

TABLE 1. Karyotypic analysis (G banding) in parental cells (H4-1) and clones

Cells	No. of PDs	No. of cells with indicated no. of chromosomes						
		44	45	46	47	48	49	50
H4-1	40	0	0	50	0	0	0	0
UBT-5	40	2	2	14	11	2	0	0
UBE6T-7	40	0	0	32	15	3	0	0
UE6E7T-12	40	0	1	45	2	0	0	0
UE7T-13	40	0	0	50	0	0	0	0
UE7T-13	80	0	0	50	0	0	0	0

Quantitative RT-PCR analysis of the *bmi-1*, TERT, E6, E7, and Nurr1 genes in UBT-5, UBE6T-7, UBE6E7T-12, and UE7T-13 cells with neuroectodermal induction at early and late PDs.

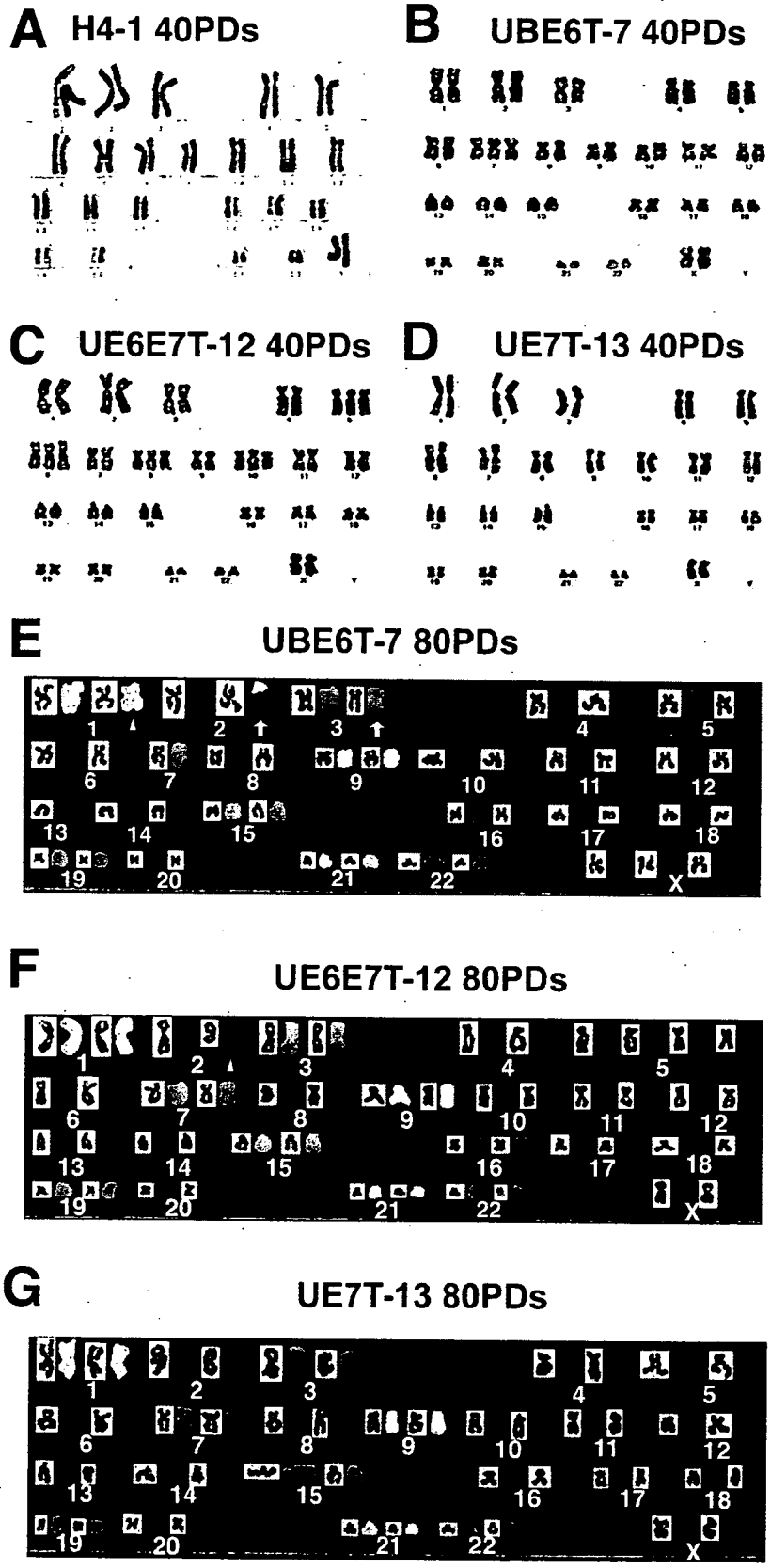

FIG. 4. Karyotypic analysis of parental and transduced cells with extended life spans. (A, B, C, and D) G-banded karyotyping. (E, F, and G) Spectral karyotyping. Metaphase spreads with structural chromosomal abnormalities were determined after the indicated number of PDs. Normal diploidy was seen in representative parental cells (A: H4-1) and UE7T-13 cells (B and G), but abnormalities were seen in UE6E7T-12 (C and F), UBE6T-7 (E), and UE7T-13 cells (D). Deletion and translocation are indicated by arrowheads and arrows, respectively.

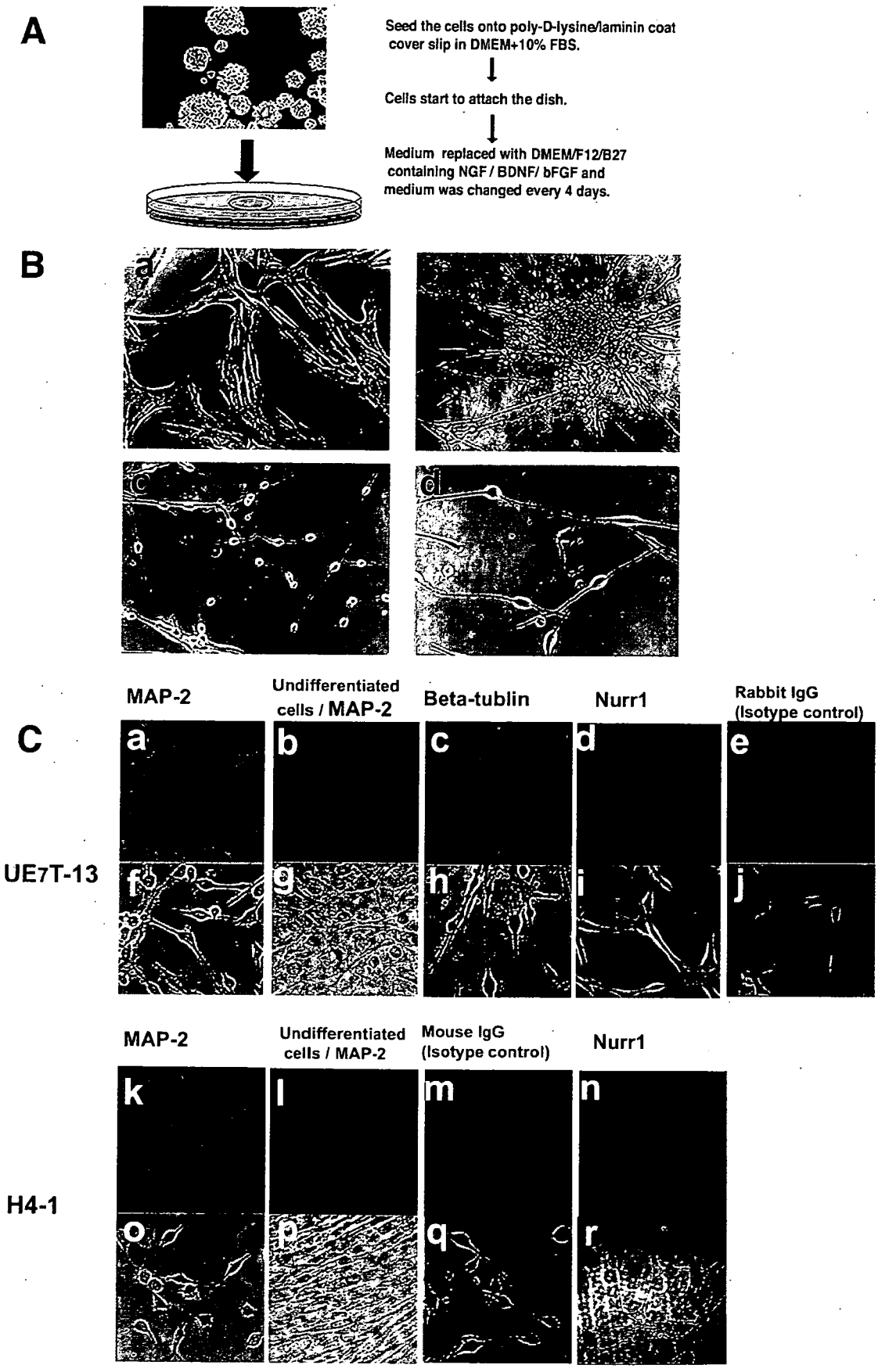
A
Seed the cells onto poly-D-lysine/laminin coat cover slip in DMEM+10% FBS.
Cells start to attach the dish.
Medium replaced with DMEM/F12/B27 containing NGF / BDNF/ bFGF and medium was changed every 4 days.
B
a
b
c
d
C
MAP-2
Undifferentiated cells / MAP-2
Beta-tublin
Nurr1
Rabbit IgG (Isotype control)
UE7T-13
a
b
c
d
e
f
g
h
i
j
MAP-2
Undifferentiated cells / MAP-2
Mouse IgG (Isotype control)
Nurr1
H4-1
k
l
m
n
o
p
q
r

TABLE 2. Genes regulated under neuronally differentiated conditions

Probe set	Description	Flag (N/C)[a]	Normalized value[b]	Fold change
Increased				
204621_s_at	Nurr1 (Nuclear receptor subfamily 4 group A member 2)	P/(A)	26.1	26.1
210663_s_at	Kynurenidase (L-kyurenine hydrolase)	P/(A)	60.7	9.6
204430_s_at	Solute carrier family 2 (facilitated glucose/fructose transporter), member 5	P/(A)	9.3	9.3
205921_s_at	Solute carrier family 6 (neurotransmitter transporter, taurine), member 6	P/(A)	6.2	6.2
205156_s_at	ACCN2 (amiloride-sensitive cation channel 2, neuronal)	P/(A)	4.1	3.4
204846_at	Ceruloplasmin (ferroxidase)	P/(A)	12.2	2.6
202507_s_at	Synaptosome-associated protein, 25 kDa	P/(A)	1.5	1.5
205792_at	WNT1-inducible signaling pathway protein 2	P/(P)	12.4	12.4
213425_s_at	WNT5A (wingless-type MMTV[c] integration site family, member 5A)	P/(P)	4.3	7.1
207594_s_at	Synaptojanin 1	P/(P)	3.3	6.1
211806_s_at	Potassium inwardly rectifying channel	P/(A)	2.5	2.5
211592_s_at	Calcium channel, voltage-dependent, L type	P/(A)	0.9	2.3
214933_at	Calcium channel, voltage-dependent, P/Q type	P/(A)	1.0	1.4
Decreased				
214081_at	Tumor endothelial marker 7	A/(P)	0.2	−19.5
209287_s_at	Cdc42 effector protein	A/(P)	0.1	−11.0
206898_at	Cadoherin 19, type 2	A/(P)	0.9	−7.1
205132_at	Actin alpha, cardiac muscle	A/(P)	0.1	−7.0
204736_s_at	Chondroitin 4-sulfotransferase	A/(P)	0.3	−5.0
209652_s_at	Placental growth factor, VEGF-related protein	A/(P)	1.0	−3.2
215177_s_at	Integrin alpha 6	A/(P)	0.5	−2.6

[a] N, neuronally differentiated UE7T-13 cells; C, undifferentiated UE7T-13 cells; P, judged to be "present" (expressed) in neuronally differentiated UE7T-13 cells; A, judged to be "absent" (not expressed) in undifferentiated UE7T-13 cells.
[b] The normalized values were calculated from data obtained in UE7T-13 cells as described in Material and Methods.
[c] MMTV, mouse mammary tumor virus.

We also performed an additional quantitative RT-PCR experiment to monitor the expression levels of the hTERT, *bmi-1*, E6, and E7 genes as well as the Nurr1 gene, during the neuronal differentiation of UBT-5, UBE6T-7, UE6E7T-12, and UE7T-13 cells (Table 3). The expression of the hTERT, E6, and E7 genes did not decrease and remained at a high level in neuronally differentiated cells. The *bmi-1* gene, on the other hand, was down-regulated. The Nurr-1 gene, a neuron marker, was significantly increased by neural induction, as expected. Although the hTERT, E6, and E7 genes were continuously strongly expressed during differentiation, the phenotype of the cells did not revert to an undifferentiated state and continued to exhibit neuronal phenotypes, even when bFGF, NGF, and BDNF were removed from the culture media.

DISCUSSION

Prolongation of the life span of human marrow stromal cells by *bmi-1*. This study was undertaken to investigate whether the life span of human marrow stromal cells, a candidate source of cells for therapy, can be prolonged by a cell-cycle associated molecule(s). Introduction of *bmi-1*, one of the polycomb group genes, clearly down-regulated p16, which is gradually induced as the number of PDs increases, and thus increases dephosphorylated Rb, resulting in the cell's escape from growth arrest or premature senescence, as we intended. This down-regulation of p16 is thought to be mediated via direct binding of *bmi-1* to the *cis*-regulatory element of p16, and thus the binding should be affected by the methylation status or chromatin structure of this *cis*-regulatory element. At the very least, *bmi-1* is functional in terms of decreasing p16 in human stromal cells, and the decrease in p16 leads to escape from premature senescence. This *bmi-1* effect on the cell life span has also been reported in human mammary epithelial cells (9), where it occurs via escape from replicative senescence by induction of telomerase activation; however, this effect of *bmi-1* on telomerase activation was not detected in our experimental human stromal cell system. In other words, *bmi-1* enables human stromal cells to escape from premature senescence but not replicative senescence.

The lack of change in phenotypes of *bmi-1*-transduced cells, for example, in their differentiation abilities, growth rates, cell surface markers, and gene expression profiles, is rather surprising, because *bmi-1* suppresses p16 protein and has been identified as a c-Myc-cooperating gene in murine B- and T-cell lymphomas (15, 37). A critical target of *bmi-1* is the *Ink4a* locus, which encodes p16 and p19 (p14 in humans) (14). In-

FIG. 5. Neuroectodermal differentiation of bone marrow stromal cells. (A) Scheme of the neuronal differentiation system. (B) Four phase-contrast microscopic images of UE7T-13 cells are shown. (a) Undifferentiated state. (b) Neuronally differentiated cells that had spread out to clusters. (c and d) Higher magnification of neuronally differentiated cells. (C) Fluorescence immunohistochemical analysis of undifferentiated UE7T-13 cells (b, g, l, and p) and neuronally differentiated cells (a, c to f, h to k, n to o, q, and r). (a, b, k, and l) MAP-2; (c) tubulin 3; (d and n) Nurr1. PE-conjugated anti-rabbit immunoglobulin G (IgG) (e) and fluorescein isothiocyanate-conjugated anti-mouse immunoglobulin antibody (m) were used as negative controls. (f, g, h, i, j, o, p, q, and r) Phase-contrast microscopic findings. All images were obtained with a laser scanning confocal microscope. (a to j) UE7T-13 cells; (k to r) H4-1 cells.

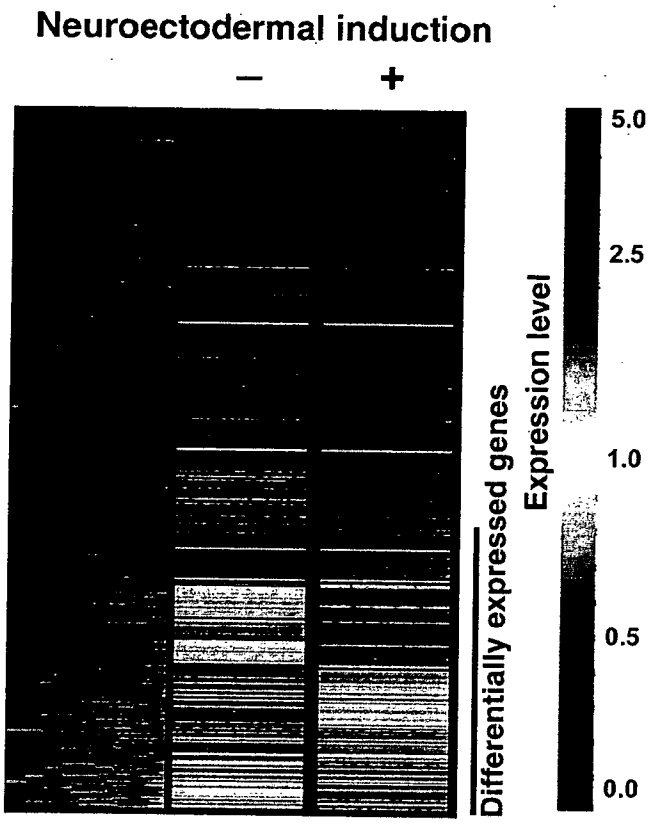

FIG. 6. Comparison between the gene profiles of neuroectodermal differentiated cells and undifferentiated cells. Gene expression levels in undifferentiated cells (−) and neuronally differentiated cells (+) are shown by the rows of colored bars that represent one gene. The color bars reflect the magnitude of the response for each gene according to the scale shown on the right. Differentially expressed genes are indicated by a vertical line on the right. The raw data from the gene chip analysis are available at the GEO database with accession number GSE2110 or our laboratory's website (http://1954.jukuin.keio.ac.jp/umezawa/chip/mori).

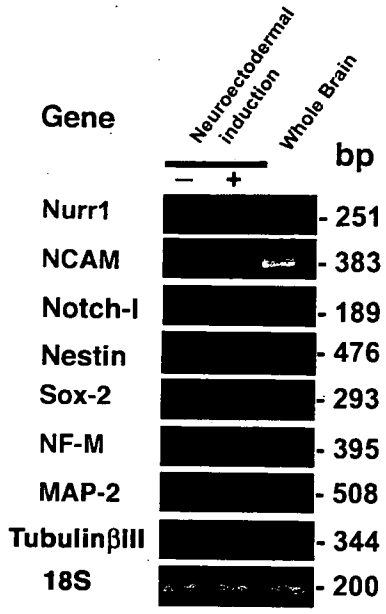

FIG. 7. RT-PCR analysis of expression of neuron-associated genes confirmed the gene chip data. RT-PCR analyses of RNAs from undifferentiated UE7T-13 cells, neuronally differentiated UE7T-13 cells, and human total brain were performed with primers that react with the human genes encoding MAP-2, tubulin 3, NF-M, Notch-1, NCAM, Sox-2, Nestin, and Nurr1. The signals of the 18S gene are approximately the same, indicating an equivalent input for all samples. Most of the neuron-associated genes were expressed by neuronally differentiated UE7T-13 cells and total brain cells.

terestingly, *bmi-1* is required for maintenance of adult self-renewing hematopoietic stem cells (29) and neural stem cells (25), whereas the simian virus 40 large T antigen oncogene, which prolongs the cell life span, interferes with the differentiation program and transforms cells. The human marrow-derived stromal cells transfected with simian virus 40 large T antigen (12) did not exhibit contact inhibition in vitro and formed tumors within a month when implanted into nude mice (data not shown).

Transdifferentiation of human mesoderm-derived cells into a functional neuronal lineage. This study was also conducted to determine whether prolongation of the cell life span by hTERT and *bmi-1*, E6, or E7 would predominate over neurogenic differentiation of marrow stromal cells in vitro. In contrast to our previous study of neurogenic differentiation of immortalized murine marrow-derived stromal cells (22) by demethylating agents, the transdifferentiation of the human stromal cells was limited to neurons, but not astrocytes or oligodendrocytes. This was probably due to the developmentally logical protocol we employed in this study: use of bFGF, NGF, BDNF, and laminin-ornithine coating. The idea for the neuronal differentiation protocol without 5-azacytidine arose from reports of the following: NGF and BDNF support neuron survival and growth (4), and bFGF induces initial differentiation of neural precursor cells and activates transcription factors related to the differentiation of neural precursor cells and embryonic stem cells (19, 31).

The extremely high level of expression of dopaminergic neuron-associated genes, such as *nurr1* and *wnt5a*, in the neuronally differentiated stromal cells, which we accidentally found by the GeneChip analysis and confirmed by RT-PCR, is surprising. *wnt5a* and *nurr1* are involved in the differentiation of midbrain precursors into dopaminergic neurons (20, 39). Although further analysis of functionally differentiated cells is beyond the scope of this study, it is quite interesting that dopaminergic neurons can be generated from marrow-derived stromal cells, since one of the target cells for regenerative medicine is dopaminergic neurons.

Are marrow stromal cells traced back to their default state, i.e., neural lineage, by neurotrophic factors? The mechanism of the transdifferentiation from marrow stromal cells to neuronal cells remains unresolved. It must be emphasized that the GeneChip analysis showed that the change in gene expression during differentiation is global and drastic: the differentiated cells no longer exhibited the profile of mesenchymal cells or the biphenotypic pattern of neuronal and mesenchymal cells. Contamination of human stromal cell cultures by neural precursor cells is inconceivable, because the cells were subcloned several times after gene transduction and exhibited mesenchymal phenotypes after subcloning. Our previous study of murine stromal cells clearly showed that osteoblasts capable of mem-

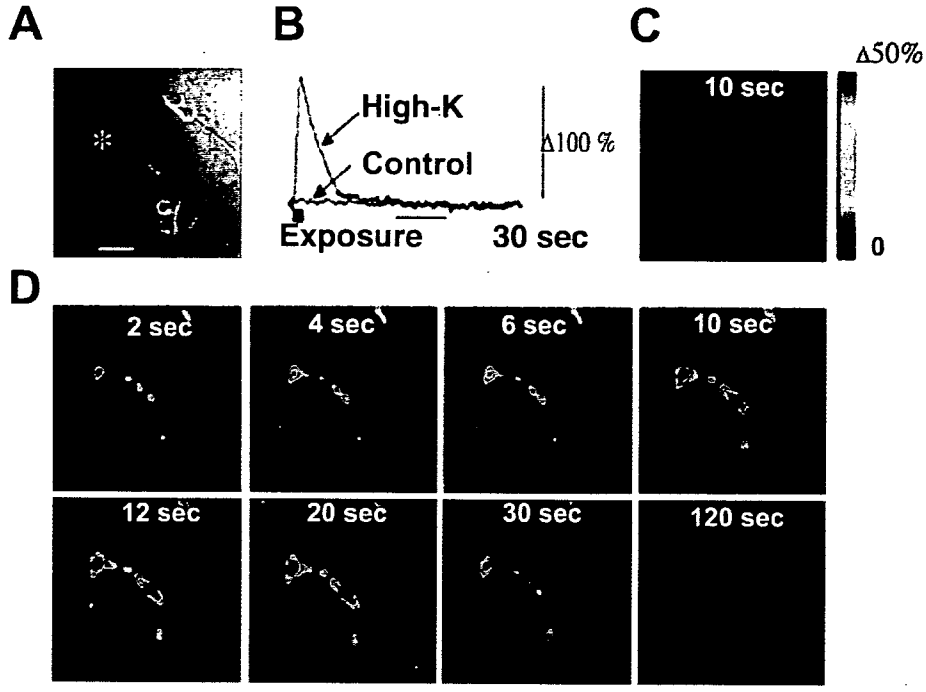

FIG. 8. Calcium imaging of neuronally differentiated stromal cells. (A) Phase-contrast photomicrograph of neuronally differentiated UE7T-13 cells. (B) The cell indicated by the asterisk in panel A showed rapid and reversible calcium uptake in response to high-potassium stimulation (red line; 115%), but simply changing the extracellular solution to the normal Tyrode's solution did not result in any calcium uptake (control; black line). Images obtained at 10 seconds after the high-potassium stimulation (D) and in the control (C). Rapid and reversible calcium uptake in response to high-potassium stimulation was observed in the four cells within this field.

TABLE 3. Quantitative RT-PCR analyses of the *bmi-1*, TERT, E6, E7, and Nurr1 genes in UBT-5, UBE6T-7, UBE6E7T-12, and UE7T-13 cells with neuroectodermal induction at early and late PDs

Cells/infected genes	No. of PDs	NI[a]	Expression level of genes[b]				
			bmi-1	TERT	E6	E7	Nurr1
UBT-5/Bmi1 and TERT	40	−	2.44	0.56			0.01
	75	−	2.13	0.48			0.02
	40	+	0.88	1.93			0.90
	75	+	0.73	6.47			1.17
UBE6T-7/*bmi-1*, E6, E7, and TERT	50	−	2.31	0.04	0.61		0.02
	120	−	0.55	0.29	0.21		0.02
	50	+	0.69	0.15	0.40		1.83
	120	+	0.15	1.18	0.87		2.69
UE6E7T-12/E6, E7, and TERT	33	−		0.35	0.62	0.28	0.02
	130	−		0.55	0.67	0.40	0.01
	33	+		0.62	4.05	1.49	2.91
	130	+		0.96	2.88	1.48	4.05
UE7T-13/E7 and TERT	33	−		0.63		1.22	0.01
	130	−		0.49		0.87	0.01
	33	+		1.17		1.01	0.78
	130	+		2.06		3.00	8.03

[a] NI, neuroectodermal induction; +, with NI; −, without NI.

[b] Cells removed from the flask bottom were placed on a coverslip coated with laminin-polylysin. One day after cell passage, the medium was replaced with B27-supplemented Dulbecco's modified Eagle's medium-F12 containing 20 ng/ml of BDNF, 10 ng/ml of bFGF, and 50 ng/ml of NGF to promote neuroectodermal differentiation. RNA was extracted from the cells for quantitative RT-PCR analysis 7 days after induction. The mRNA levels were normalized using the GAPDH gene as a housekeeping gene.

branous ossification are likely to differentiate into neuronal lineages but that adipocytes do not (22). The craniofacial membranous bones develop from the neural crest, which is of ectodermal origin. Our finding of in vitro differentiation from mesoderm- to ectoderm-derived cells in this study may be the opposite of the developmental process, i.e., from ectoderm- to mesoderm-derived cells. Development naturally progresses from neural crest cells to terminally differentiated osteoblasts (28). Converting differentiated osteoblasts or marrow stromal cells to neuronal cells, a key future task for any cell-based therapy, would thus oppose the usual direction of cell differentiation. This can now be achieved by exposing stromal cells to neurotrophic factors, at least in vitro.

Are human marrow stromal cells with an extended life span available for cell-based therapy? Human stromal cells transduced with hTERT and *bmi-1*, E6, or E7 did not transform according to the classical criteria: they did not generate tumors in immunosuppressed NOD-SCID-interleukin 2 receptor knockout mice, they did not form foci in vitro, and they stopped dividing after confluence (data not shown). However, we cannot rule out the possibility that gene-transduced stromal cells might become tumorigenic in patients several decades after cell therapy. We believe that these gene-modified stromal cells may be used to supply defective enzymes to patients with genetic metabolic diseases, such as neuro-Gaucher disease, Fabry disease, and mucopolysaccharidosis, which have a poor prognosis and are sometimes lethal. The "risk-versus-benefit" balance is essential when applying these gene-modified cells clinically, and the "risk" or "drawback" in this case is transformation of implanted cells.

hTERT is normally expressed in stem cells and in over 90% of human cancers. Ectopic expression of telomerase is sufficient to prevent telomere shortening and can thereby promote indefinite proliferation in human foreskin fibroblasts (5). Several stromal cell strains with extended life spans and maintenance of differentiation capability, such as UBT5, UBE6T7, UE6E7T-12, UE7T-13, and UE6E7-16 cells, were developed based on the above notion. UE6E7-16 cells not transduced with hTERT have a longer life span but enter a "crisis" period in culture at 67 PDs. "Crisis" is the stage in which widespread death occurs in a population of cultured cells or when karyotypic instability develops as a result of fusion of telomere ends, after the cells manage to circumvent senescence or initial blockades. Human cells transduced with *bmi-1* or E6 and E7 alone enter a "crisis," and the cells that spontaneously circumvent premature senescence without gene induction enter replicative senescence. Replicative senescence or crisis may be a tumor suppressor mechanism that avoids the risk of cell transformation after implantation of cells as a source for cell-based therapy.

Even when cells transduced with nononcogenic genes are used for cell-based therapy, the cases of leukemia in SCID patients treated with gene-modified lymphocytes must be taken into account (3). The infected virus genome was integrated into the LMO2 locus in the leukemia cases and resulted in induction of the oncogenic LMO2 gene. Because of these failures, it will take time before gene-modified cells can be used for regenerative medicine. Inhibition of the p16/Rb pathway is sufficient to prolong the life span of cells in cultures of marrow-derived stroma, as shown in this study. The p16/Rb pathway was activated in marrow-derived stromal cells in vitro, the same as in mammary epithelial cells and hepatocytes, but not in foreskin fibroblasts (21). The development of an appropriate culture system without gene transduction to neutralize the p16/Rb braking system, i.e., nonstress medium, will be essential for cell therapy and further experiments.

ACKNOWLEDGMENTS

We express our sincere thanks to K. Segawa, S. Matsumoto, Y. Okayama, S. Okuyama, and S. Ikeuchi for support throughout the work and to Y. Nakamura, N. Hida, N. Hashimoto, and T. Inomata for providing expert technical assistance. We are grateful to D. A. Galloway (FHCRC, Seattle, Wash.) for pLXSN-16E7 and to Y. Takeuchi (Chester Beatty Laboratories, ICR, United Kingdom) for the FLYA13 cells.

This work was supported in part by a special grant for Advanced Research on Cancer from the Ministry of Education, Culture, Sports, Science, and Technology (MEXT) of Japan to T.K. and A.U.; a grant from MEXT to A.U.; Health and Labour Sciences Research Grants to A.U.; and a grant from the Organization for Pharmaceutical Safety and Research to A.U.

REFERENCES

1. **Ahn, J. I., K. H. Lee, D. M. Shin, J. W. Shim, J. S. Lee, S. Y. Chang, Y. S. Lee, M. J. Brownstein, and S. H. Lee.** 2004. Comprehensive transcriptome analysis of differentiation of embryonic stem cells into midbrain and hindbrain neurons. Dev. Biol. **265**:491–501.
2. **Allan, E. H., P. W. Ho, A. Umezawa, J. Hata, F. Makishima, M. T. Gillespie, and T. J. Martin.** 2003. Differentiation potential of a mouse bone marrow stromal cell line. J. Cell Biochem. **90**:158–169.
3. **Allsopp, R. C., H. Vaziri, C. Patterson, S. Goldstein, E. V. Younglai, A. B. Futcher, C. W. Greider, and C. B. Harley.** 1992. Telomere length predicts replicative capacity of human fibroblasts. Proc. Natl. Acad. Sci. USA **89**: 10114–10118.
4. **Batchelor, P. E., G. T. Liberatore, M. J. Porritt, G. A. Donnan, and D. W. Howells.** 2000. Inhibition of brain-derived neurotrophic factor and glial cell line-derived neurotrophic factor expression reduces dopaminergic sprouting in the injured striatum. Eur. J. Neurosci. **12**:3462–3468.
5. **Bodnar, A. G., M. Ouellette, M. Frolkis, S. E. Holt, C. P. Chiu, G. B. Morin, C. B. Harley, J. W. Shay, S. Lichtsteiner, and W. E. Wright.** 1998. Extension of life-span by introduction of telomerase into normal human cells. Science **279**:349–352.
6. **Brazelton, T. R., F. M. Rossi, G. I. Keshet, and H. M. Blau.** 2000. From marrow to brain: expression of neuronal phenotypes in adult mice. Science **290**:1775–1779.
7. **Brewer, G. J., J. R. Torricelli, E. K. Evege, and P. J. Price.** 1993. Optimized survival of hippocampal neurons in B27-supplemented Neurobasal, a new serum-free medium combination. J. Neurosci Res. **35**:567–576.
8. **Castelo-Branco, G., J. Wagner, F. J. Rodriguez, J. Kele, K. Sousa, N. Rawal, H. A. Pasolli, E. Fuchs, J. Kitajewski, and E. Arenas.** 2003. Differential regulation of midbrain dopaminergic neuron development by Wnt-1, Wnt-3a, and Wnt-5a. Proc. Natl. Acad. Sci. USA **100**:12747–12752.
9. **Dimri, G. P., J. L. Martinez, J. J. Jacobs, P. Keblusek, K. Itahana, M. Van Lohuizen, J. Campisi, D. E. Wazer, and V. Band.** 2002. The *bmi-1* oncogene induces telomerase activity and immortalizes human mammary epithelial cells. Cancer Res. **62**:4736–4745.
10. **Faux, C. H., A. M. Turnley, R. Epa, R. Cappai, and P. F. Bartlett.** 2001. Interactions between fibroblast growth factors and Notch regulate neuronal differentiation. J. Neurosci. **21**:5587–5596.
11. **Gojo, S., N. Gojo, Y. Takeda, T. Mori, H. Abe, S. Kyo, J. Hata, and A. Umezawa.** 2003. In vivo cardiovasculogenesis by direct injection of isolated adult mesenchymal stem cells. Exp. Cell Res. **288**:51–59.
12. **Hacein-Bey-Abina, S., C. Von Kalle, M. Schmidt, M. P. McCormack, N. Wulffraat, P. Leboulch, A. Lim, C. S. Osborne, R. Pawliuk, E. Morillon, R. Sorensen, A. Forster, P. Fraser, J. I. Cohen, G. de Saint Basile, I. Alexander, U. Wintergerst, T. Frebourg, A. Aurias, D. Stoppa-Lyonnet, S. Romana, I. Radford-Weiss, F. Gross, F. Valensi, E. Delabesse, E. Macintyre, F. Sigaux, J. Soulier, L. E. Leiva, M. Wissler, C. Prinz, T. H. Rabbitts, F. Le Deist, A. Fischer, and M. Cavazzana-Calvo.** 2003. LMO2-associated clonal T cell proliferation in two patients after gene therapy for SCID-X1. Science **302**: 415–419.
13. **Imabayashi, H., T. Mori, S. Gojo, T. Kiyono, T. Sugiyama, R. Irie, T. Isogai, J. Hata, Y. Toyama, and A. Umezawa.** 2003. Redifferentiation of dedifferentiated chondrocytes and chondrogenesis of human bone marrow stromal cells via chondrosphere formation with expression profiling by large-scale cDNA analysis. Exp. Cell Res. **288**:35–50.
14. **Jacobs, J. J., K. Kieboom, S. Marino, R. A. DePinho, and M. van Lohuizen.** 1999. The oncogene and Polycomb-group gene bmi-1 regulates cell proliferation and senescence through the ink4a locus. Nature **397**:164–168.
15. **Jacobs, J. J., B. Scheijen, J. W. Voncken, K. Kieboom, A. Berns, and M. van Lohuizen.** 1999. *bmi-1* collaborates with c-Myc in tumorigenesis by inhibiting c-Myc-induced apoptosis via INK4a/ARF. Genes Dev. **13**:2678–2690.
16. **Jiang, Y., D. Henderson, M. Blackstad, A. Chen, R. F. Miller, and C. M. Verfaillie.** 2003. Neuroectodermal differentiation from mouse multipotent adult progenitor cells. Proc. Natl. Acad. Sci. USA **100**(Suppl. 1):1854–1860.
17. **Kageyama, R., and T. Ohtsuka.** 1999. The Notch-Hes pathway in mammalian neural development. Cell Res. **9**:179–188.
18. **Kageyama, R., T. Ohtsuka, and K. Tomita.** 2000. The bHLH gene Hes1 regulates differentiation of multiple cell types. Mol. Cell **10**:1–7.
19. **Kalyani, A. J., T. Mujtaba, and M. S. Rao.** 1999. Expression of EGF receptor and FGF receptor isoforms during neuroepithelial stem cell differentiation. J. Neurobiol. **38**:207–224.
20. **Kim, J. H., J. M. Auerbach, J. A. Rodriguez-Gomez, I. Velasco, D. Gavin, N. Lumelsky, S. H. Lee, J. Nguyen, R. Sanchez-Pernaute, K. Bankiewicz, and R. McKay.** 2002. Dopamine neurons derived from embryonic stem cells function in an animal model of Parkinson's disease. Nature **418**:50–56.
21. **Kiyono, T., S. A. Foster, J. I. Koop, J. K. McDougall, D. A. Galloway, and A. J. Klingelhutz.** 1998. Both Rb/p16INK4a inactivation and telomerase activity are required to immortalize human epithelial cells. Nature **396**:84–88.
22. **Kohyama, J., H. Abe, T. Shimazaki, A. Koizumi, K. Nakashima, S. Gojo, T. Taga, H. Okano, J. Hata, and A. Umezawa.** 2001. Brain from bone: efficient "meta-differentiation" of marrow stroma-derived mature osteoblasts to neurons with Noggin or a demethylating agent. Differentiation **68**:235–244.
23. **Le, W. D., P. Xu, J. Jankovic, H. Jiang, S. H. Appel, R. G. Smith, and D. K. Vassilatis.** 2003. Mutations in NR4A2 associated with familial Parkinson disease. Nat. Genet. **33**:85–89.
24. **Makino, S., K. Fukuda, S. Miyoshi, F. Konishi, H. Kodama, J. Pan, M. Sano, T. Takahashi, S. Hori, H. Abe, J. Hata, A. Umezawa, and S. Ogawa.** 1999. Cardiomyocytes can be generated from marrow stromal cells in vitro. J. Clin. Investig. **103**:697–705.
25. **Molofsky, A. V., R. Pardal, T. Iwashita, I. K. Park, M. F. Clarke, and S. J. Morrison.** 2003. *bmi-1* dependence distinguishes neural stem cell self-renewal from progenitor proliferation. Nature **425**:962–967.
26. **Ochi, K., G. Chen, T. Ushida, S. Gojo, K. Segawa, H. Tai, K. Ueno, H. Ohkawa, T. Mori, A. Yamaguchi, Y. Toyama, J. Hata, and A. Umezawa.** 2003. Use of isolated mature osteoblasts in abundance acts as desired-shaped